Imaging Practice and Radiation Protection in Pediatric Radiology

Conventional Radiography

Michael Seidenbusch
Veronika Rösenberger
Karl Schneider

Springer

Imaging Practice and Radiation Protection in Pediatric Radiology

Michael Seidenbusch
Veronika Rösenberger • Karl Schneider

Imaging Practice and Radiation Protection in Pediatric Radiology

Conventional Radiography

Springer

Michael Seidenbusch
Department of Paediatric Radiology
Dr. von Hauner Children's Hospital
University of Munich
Munich
Germany

Karl Schneider
Department of Paediatric Radiology
Dr. von Hauner Children's Hospital
University of Munich
Munich
Germany

Veronika Rösenberger
Department of Paediatric Radiology
Dr. von Hauner Children's Hospital
University of Munich
Munich
Germany

ISBN 978-3-030-18502-2 ISBN 978-3-030-18504-6 (eBook)
https://doi.org/10.1007/978-3-030-18504-6

This Springer imprint is published by the registered company Springer Nature Switzerland AG.
The registered company address is: Gewerbestrasse 11, 6330 Cham, Switzerland

This book is dedicated to
Karla
with my sincerest thanks for all her love and patience
and to
my parents
for rendering possible my path of life
and my professional history.

Munich, Summer 2019

Michael Seidenbusch

Foreword

In neonates, organs and tissues of infants and young children are localized closer to each other than in adults and—according to radio-biological investigations—children are more sensitive to ionizing radiation. Quality criteria for diagnostic radiographic imaging needed to be specifically adapted to paediatric radiology. After the important work in 1979 of *Rosenstein* on the calculation of organ doses in paediatric age groups, this book closes a wide gap on this topic.

The authors, internationally renowned in the field, provide new normalized organ doses for conventional paediatric X-ray examinations in all age groups. Although the mathematical phantoms had some inaccuracies concerning the location, size, and shape of the organs in the different age groups, the anatomy of the developing child is detailed enough to get reliable dose calculations. Clinical indications, different field settings, exposure parameters, image quality criteria, and normalized radiation doses have been investigated. The combination of these criteria, especially with various field settings, offers new aspects of dose reduction and risk calculation.

The book is well organized with clear figures and similar structure and formation of the tables for all investigated regions.

Imaging practice and radiation protection should be the reference tool for everybody who works in paediatric radiology.

Don't forget, children are our future.

Cologne, Germany — Gabriele Benz-Bohm

Preface

"Es hat nie einen Mann gegeben, der für die Behandlung von Einzelheiten so begabt gewesen wäre. Wenn er sich mit den kleinsten Dingen abgab, so tat er das in der Überzeugung, daß ihre Vielheit die großen zuwege bringt."—"There has never been a man who was more capable to address details. If he had to do with the minor details he did it believing that a lot of minor things would produce the great ones."

Friedrich II. about Friedrich Wilhelm I., both kings of Prussia

Children are amongst the most radiation-sensitive living creatures on earth. Thus, radiation protection of young patients might be one of the most important issues in paediatric diagnostic radiology. On ethical grounds, children also need greater protection against diseases compared to adults. Thus, imaging of the child in paediatric radiology is an essential part of medicine. But trying to optimize radiation exposure and image quality simultaneously may make the paediatric radiologist feel himself like Ulysses between Scylla and Charybdis.

Indeed, especially in paediatric radiology, there are numerous interacting exposure parameters which influence radiation exposure and image quality, a fact that makes the optimization process in paediatric radiology so complicated. The authors of this book would like to contribute some facts to help clarify this situation. This book addresses mainly to all radiologists and technologists who are involved in paediatric imaging and who wish to improve the radiation protection of children by choosing adequate field settings and exposure parameters. The book addresses also to medical physicists and epidemiologists who want to reconstruct organ doses achieved in patients during conventional paediatric X-ray examinations.

The authors are aware that they perform a balancing act when trying to bring together two quite distinct areas of paediatric radiology, the exposure technique and the radiation dosimetry, each of them comprehensive enough to fill an entire book. However, the authors believe that it is this combination that may help the reader to assess the dosimetric consequences of the applied exposure practice.

The book is divided into four parts. In the first part, a very short introduction will be given to the topics of radiation exposure and radiation risk. In the second part, a short introduction to radiation physics and radiation dosimetry will be given. However, the first two parts are no prerequisites at all for understanding the third part as the main part of this book. In the third part, a short introduction will be given on how to calculate organ doses from clinically

measured dose indicators. Each chapter in this part deals with a specific radiographic technique and provides a lot of tables subsuming clinical indications, image quality requirements, field settings, exposure parameters, and normalized organ doses which result from various field settings and exposure conditions. Finally, the fourth part of this book provides additional information on the state of the art of dose reconstruction in paediatric radiology.

In preparation for this book, the authors were greatly assisted by several people. First of all, the authors are grateful to Mrs. Corinna Hauser, to Mrs. Anna Lena Buchholz, and to Mrs. Wilma McHugh, Springer Company, for all their advice and patience. The authors want also to express their gratitude to Mrs. Saanthi Shankhararaman and Mr. Kumar Srinivasan Deepak, Springer Company, and their team for their patience and accuracy when preparing the layout of the book. Special thanks go to Prof. Dr. Stefan Milz, anatomist at the University of Munich and editor-in-chief of the Journal of Anatomy, as well as to M. A. Franz Jürgen Götz, librarian of the national library of Bavaria, for supporting the literature research. Thanks go also to our colleague Dr. med. Birgit Kammer, head of the section for paediatric radiology at Dr. von Hauner Children's Hospital, and to Mrs. Sieglinde "Sigi" Eberle, chief radiographer of the section for paediatric radiology, who have provided photographs of X-ray devices. And last but not least, the authors want to thank Mrs. Tanja Smith and Mrs. B. A. Isabella Körbl for performing the linguistic review of this book.

The authors want herewith to express their hope that this book might support a short step on the long way of radiation protection in paediatric radiology.

Munich, Germany
Summer 2019

Michael Seidenbusch
Veronika Rösenberger
Karl Schneider

Contents

Part I

Introduction

"Wir werden ja sehen, was wir sehen."—"We shall see what we will see."
***Wilhelm Conrad Röntgen,* 28.12.1895**

1 Radiation Risk and Radiation Protection in Paediatric Radiology

1.1 Paediatric Radiology

Immediately after *Wilhelm Conrad Röntgen*'s publication about X-rays[1] in December 1895 [58], the evolution of diagnostic radiology as a new medical discipline started [30], and so did the evolution of paediatric radiology. By 1896, within a very short period of time, 21 reports had been published on X-ray examinations in children [67]. Now, in rapid succession, departments for paediatric radiology were founded all over the world: In 1897, possibly for the first time ever, a department of paediatric radiology was established by the German physician and bacteriologist *Theodor Escherich* in the Anna Children's Hospital in Graz, Austria, [2, 16, 26], and in 1899, in the United States of America, the first department of paediatric radiology was founded in the Children's Hospital of Boston by the civil war surgeon *Francis Henry Brown* [8, 26]. These foundations can be traced back to the fact that, within a little while, diagnostic radiology had become an essential diagnostic tool not only in adult medicine [30] but also in paediatrics [1, 30, 57]. Nevertheless, child-specific radiological methods had still to be developed in the following decades [55, 59].

[1]In Germany, Austria, and Switzerland, the new kind of radiation discovered by *Roentgen* has been called "Röntgenstrahlung" (Roentgen rays), in other countries "x-rays" with "x" standing for "unknown".

1.2 Radiation Risk in Paediatric Radiology

At that time, typical radiographies required radiation exposures of several minutes [7, 14, 37]. Thus, radiation doses achieved in patients during X-ray examinations were about three orders of magnitude higher than today [38, 41]. As a consequence, adverse biological effects could be observed in clinical practice already within the first year of X-ray diagnostics. As an example, a case of hair-loss after a paediatric X-ray examination was described by *Daniel* [11] as an "interesting observation [of] a physiological effect of the x-rays" in April of 1896, but, of course, due to the lack of knowledge about the true nature of X-rays in former times, no correct pathomechanism could be identified.

Today, after more than 100 years of world-wide radiation research, the risks associated with ionizing radiation can be divided into deterministic and stochastic biological effects [39]. While deterministic effects do occur only after exceeding a tissue-specific threshold dose below which the effect is not observed, there is, according to the present state of research, no threshold for stochastic effects [39], of which radiation-induced cancerogenesis is the most terrifying one. Thus, since it is impossible to avoid stochastic radiation effects completely, these effects do play a crucial role in radiation protection especially in diagnostic radiology where ionizing radiations are intended to be

M. Seidenbusch et al., *Imaging Practice and Radiation Protection in Pediatric Radiology*,
https://doi.org/10.1007/978-3-030-18504-6_1

clinically applied in order to avert further deterministic pathologic damage of patients.

Unfortunately, children have to be considered as being much more radiation-sensitive than adults. Radiation exposure in children under 10 years has been assumed to increase the stochastic radiation risk by a factor of 3–4 [33]. And in fact, radio-biological investigations have shown in recent years that organs and tissues in children seem to be much more sensitive to ionizing radiation than those of adults [64, 66]. This fact is of utmost importance in paediatric radiology as most of the paediatric X-ray examinations are performed in neonates and young infants [62, 63] who may be even more radiosensitive than children of other age groups.

To add insult to injury, the collective radiation exposure of the European and US American population is mainly determined by medical imaging [13, 48, 56] and is still going up due to the increasing use of computed tomography in medical diagnostics [5]. Therefore, it can be assumed that this will also apply to children who represent a percentage of about 15–25% of the European and US American populations [20, 26]. Indeed, up to 10% of all conventional X-ray examinations are performed in children in Western Europe [17], and up to 15% in the United States [48], a lot of them in neonates and young infants [54]. Accordingly, *Brenner* et al. have warned at the beginning of the new millennium that the stochastic radiation risk of children might be considerably increased through paediatric computed tomographic (CT) examinations [3, 4]. Moreover, direct epidemiologic proof has been given recently of a significantly heightened risk for neoplastic diseases after CT examinations in the age range under 22 years [40, 52]. Nevertheless, diagnostic imaging of children by means of ionizing radiation is one of the most important diagnostic techniques in paediatrics and there is a clear common agreement that children's health is a primary consideration [65].

1.3 Radiation Protection in Paediatric Radiology

Against this background, the radiation exposure during X-ray examinations ought to be minimized especially in children and young adolescents. This requires a rational use of ionizing radiation [21–23, 28]. Today, there exist three fundamental principles of rational use of ionizing radiation in medicine [44] which are based on each other: justification, optimization, and limitation [26, 31, 35, 43, 63].

1.3.1 Justification

The fundamental and most effective principle of radiation protection in paediatric radiology is the principle of justification which represents one of the main tasks of the paediatric radiologist. Justification involves the question whether the particular procedure will actually have any benefit for the individual patient [26]. Thus, by observing the principles of efficacy [23, 26], many paediatric X-ray examinations might be avoided and replaced by alternative diagnostic procedures of similar diagnostic yield [50].

1.3.2 Optimization

If a paediatric X-ray examination is indicated according to the principle of justification, the radiation exposure ought to be kept as low as reasonably achievable. This demand has been summarized in the so-called ALARA concept, where ALARA is an acronym for the phrase "as low as reasonably achievable" [68]. This concept can be traced back to the phrase that radiation exposure should be kept "at the lowest practical level" in a report of the American National Committee on Radiation Protection (NCRP) which was published in 1954 [42, 47]. The ALARA concept may be also derived from the ALARP principle that has arisen in 1974 from legislation in the United Kingdom [51], where ALARP is the acronym for "as low as reasonably practicable".

Probably for the first time in paediatric radiology the principle of minimization was postulated by the German paediatrician *Reyher* in his paediatric radiology textbook entitled "Das Röntgenverfahren in der Kinderheilkunde" ("Roentgenology in paediatrics") [49, 57].

In Europe, systematic efforts were made in order to improve image quality and radiation exposure of patients in diagnostic radiology [46] since the 1960s. Based on these efforts and on the concept of efficacy which was defined by the World Health Organization (WHO) in 1977, *Helmut Fendel*, a paediatric radiologist at the Dr. von Hauner Children's Hospital, University of Munich, introduced a new era of radiation protection in paediatric radiology [21, 22, 24] considering the radiation doses as well as the image quality achieved during paediatric X-ray examinations [23, 25]. His publications anticipated the principles of justification and optimization introduced by the International Commission on Radiological Protection (ICRP) [31, 32]. In 1989, *Fendel* founded the so-called Lake Starnberg Group (Fig. 1.1, Table 1.1), a group of researchers of the European Society of Paediatric Radiology (ESPR) that held their meetings at the Lake Starnberg, Bavaria. In these years, efforts have been made by international working groups in order to optimize image quality and radiation exposure during conventional X-ray examinations [15, 45, 46]. After *Fendel*'s death in 1991, his successor *Karl Schneider* performed fundamental investigations on the image quality as well as the radiation dose in paediatric radiology all over Europe [61]. In 1996, the European Network of Pediatric Radiology (ENPR) that emerged from the former Lake Starnberg Group published the European Guidelines on quality criteria in paediatric radiology [9, 53]. These studies were considered in a recommendation of the German Commission for Radiation Protection [12] even many years later. In the United Kingdom, *Valmai Cook* published guidelines on the best imaging practice in paediatric imaging in 1998 [10]. The German Medical Association published in 2007 guidelines for all radiographic and fluoroscopic examinations with specific comments on the imaging procedures of paediatric patients [29], and so did the Austrian Ministry of Health [27].

Fig. 1.1 Helmut Fendel, founder of the Lake Starnberg Group, at the opening ceremony of the annual meeting of the European Society of Paediatric Radiology (ESPR), Munich 1990

Table 1.1 Members of the Lake Starnberg Group and the European Network of Paediatric Radiologists

Rosemary Arthur	Leeds, UK
Giampiero Beluffi	Pavia, Italy
Valmai Cook	London, UK
Clément Fauré ┼	Paris, France
Helmut Fendel ┼	Munich, Germany
Eldad Horwitz	Würzburg, Germany
Peter Kramer ┼	Utrecht, The Netherlands
Jean-Philippe Montagne	Paris, France
Noemi Perlmutter	Brussels Belgium
Karl Schneider	Munich, Germany
Betty Sweet	Glasgow, UK
Paul Thomas	Belfast, UK

Annotations:
┼ = deceased

1.3.3 Limitation

The concept of diagnostic reference levels (DRL) was introduced in radiation protection in 1997 [34]. This concept was developed and used for a long time in the United Kingdom. The DRL were defined as the third quartile dose values—either the entrance surface dose or the dose-area product values—received from large field stud-

ies in country. The very meaning is that radiology departments or private practices which exceed the third quartile values make at least one significant mistake in the daily routine imaging [36]. In Germany, DRL were introduced in 2003 [6] using the data from several European field studies published in European Guidelines [9] and have been revised three times, last amended in 2016 [60]. In the meantime, dose reference levels of many European countries have been published by the national authorities [9, 18, 19]. However, the DRL were not implemented in all European member states. Furthermore, they differ by a factor between 5 and 15 for chest X-rays which is the most radiographic examination in paediatrics. The reasons are diverse, but can be mainly attributed to ignore the recommendations on good radiographic practice outlined in the European guidelines on quality criteria for diagnostic radiographic images in paediatrics [9].

References

1. Benz-Bohm G, Richter E. Chronik der Kinderradiologie. Berlin, Heidelberg: Springer; 2012.
2. Benz-Bohm G, Stöver B, Riccabona M. 50 years Gesellschaft für Pädiatrische Radiologie—a challenge. Fortschr Röntgenstr. 2013;185:807–9.
3. Brenner DJ. Estimating cancer risks from pediatric CT: going from the qualitative to the quantitative. Pediatr Radiol. 2002;32:228–31.
4. Brenner DJ, Elliston CD, Hall EJ, Berdon WE. Estimated risks of radiation-induced fatal cancer from pediatric CT. AJR. 2001;176:289–96.
5. Brenner DJ, Hall EJ. Computed tomography: an increasing source of radiation exposure. N Engl J Med. 2007;357:2277–84.
6. Brix G. Bekanntmachung der diagnostischen Referenzwerte für radiologische und nuklearmedizinische Untersuchungen: Bundesamt für Strahlenschutz, Salzgitter; 2003.
7. Bürgerspital Basel. Jahresbericht pro 1899. Basel; 1899.
8. Caffey J. The first sixty years of pediatric roentgenology in the United States—1896 to 1956. AJR. 1956;76:437–54.
9. Commission of the European Communities. European guidelines on quality criteria for diagnostic radiographic images in paediatrics. EUR 16261, SBN 92-827-7843-6; 1996.
10. Cook JV, Shah K, Pablot S, Kyriou J, Pettett A, Fitzgerald M. Guidelines on best practice in the x-ray imaging of children. A manual for all x-ray departments. London: Queen Mary's Hospital for Children, Surrey, and The Radiological Protection Centre; 1998.
11. Daniel J. The x-rays. Science. 1896;3:562–3.
12. Deutsche Strahlenschutzkommission. Bildgebende Diagnostik beim Kind—Strahlenschutz, Rechtfertigung und Effektivität. Empfehlung der Strahlenschutzkommission, Deutschland; 2006.
13. Deutscher Bundestag, 18. Wahlperiode. Unterrichtung durch die Bundesregierung. Umweltradioaktivität und Strahlenbelastung im Jahr 2014. Drucksache 18/9600; 2016.
14. Dommann M. Durchsicht, Einsicht, Vorsicht. Eine Geschichte der Röntgenstrahlen, 1896-1963. Zürich: Chronos-Verlag; 2003.
15. Drexler G, Eriskat H, Schibilla H, Haybittle JL, Secretan LF. Criteria and methods for quality assurance in medical x-ray diagnosis. Br J Radiol. 1985;Suppl 18.
16. Escherich T. Die diagnostische Verwertung des Röntgenverfahrens bei Untersuchung der Kinder. Fortschr Röntgenstr. 1899;3:119.
17. European Commission. Radiation Protection 154. European guidance on estimating population doses from medical x-ray procedures. Directorate-General for energy and transport, Directorate H—Nuclear energy, Unit H.4—Radiation protection; 2008.
18. European Commission. Radiation Protection 180. Diagnostic reference levels in thirty-six European countries. Directorate-General for energy, Directorate D—Nuclear safety & fuel cycle, Unit D.3—Radiation protection; 2014.
19. European Commission. Radiation Protection 185. European guidelines on diagnostic reference levels for paediatric imaging. Directorate-General for Energy, Directorate D—Nuclear Energy, Safety and ITER, Unit D3—Radiation Protection and Nucl Saf; 2018.
20. Eurostat. Population structure and ageing. ISSN 2443-8219; 2016.
21. Fendel H. Die zehn Gebote des Strahlenschutzes bei der Röntgenuntersuchung im Kindesalter. Pädiat Prax. 1976;17:339–46.
22. Fendel H, Schneider K. Vernünftige diagnostische Bildgebung in der Kinderurologie. Krankenhaus-Arzt. 1988;61:513–22.
23. Fendel H, Schneider K, Bakowski C, Glas J, Drews K, Kohn MM. The efficacy of diagnostic radiation in paediatrics. Report of the Federal Ministery for Environment, Environment Protection and Reactor Safety of the Federal Republic of Germany, BMU-1987-161; 1987.
24. Fendel H, Stieve FE, editors. Radiation protection in pediatric radiology. NCRP report 68; 1983.
25. Fendel H, Stieve FE, editors. Vernünftige diagnostische Bildgebung bei Kindern. Bericht einer Studiengruppe der Weltgesundheitsorganisation. Berlin: Hoffmann Verlag; 1990.
26. Fendel H, Sweet EM, Thomas PS, editors. The status of paediatric radiology in Europe. Berlin: Schering AG; 1991. ISBN 3-921817-43-9.

27. Fotter R, Sinzig M, Jost G, Unterweger O, Weissensteiner S. Qualitätskriterien für Röntgenaufnahmen bei Kindern. Ein Leitfaden der AG Kinderradiologie: Österreichisches Bundesministerium für Gesundheit.
28. Fuchs W. Simple recommendations on how to avoid radiation harm. Western Electrician. 1896;12.
29. German Medical Association. Guidelines of the German Medical Association for quality assurance in diagnostic radiology. 2007.
30. Gocht H. Die Röngten-Literatur. II. Teil: Sachregister. Stuttgart: Enke Verlag; 1912.
31. International Commission on Radiological Protection. Protection against ionizing radiation from external sources. ICRP report 15; 1969.
32. International Commission on Radiological Protection. Recommendations of the International Commission on Radiological Protection. ICRP publication 26; 1977.
33. International Commission on Radiological Protection. 1990 recommendations of the International Commission on Radiological Protection. ICRP publication 60; 1990.
34. International Commission on Radiological Protection. Radiological protection and safety in medicine. ICRP publication 73; 1997.
35. International Commission on Radiological Protection. Radiological protection in paediatric diagnostic and interventional radiology. ICRP publication 121; 2013.
36. International Commission on Radiological Protection. Diagnostic reference levels in medical imaging. ICRP publication 135; 2017.
37. Kaufmann HJ, Ringertz H, Sweet E, editors. The first 30 years of the ESPR. The history of pediatric radiology in Europe. Berlin, Heidelberg: Springer; 1993. ISBN 978-3-540-56541-3.
38. Kemerink M, Dierichs TJ, Dierichs J, Huynen HJM, Wildberger JE, van Engelshoven JMA, Kemerink GJ. Characteristics of a first-generation x-ray system. Radiology. 2011;259:534–9.
39. Little MP. Risks associated with ionizing radiation. Br Med Bull. 2003;68:259–75.
40. Mathews JD, Forsythe AV, Brady Z, Butler MW, Goergen SC, Byrnes GB, Giles GG, Wallace AB, Anderson PR, Guiver TA, McGale P, Cain TM, Dowty JG, Bickerstaffe AC, Darby SC. Cancer risk in 680 000 people exposed to computed tomography scans in childhood or adolescence: data linkage study of 11 million Australians. BMJ. 2013;346:f2360.
41. Melo DR, Miller DL, Chang L, Moroz B, Linet MS, Simon SL. Organ doses from diagnostic medical radiography—trends over eight decades (1930 to 2010). Health Phys. 2016;111:235–55.
42. Miller DL, Schauer D. The ALARA principle in medical imaging. AAPM Newslett. 2015;40:38–40.
43. Moores BM. A review of the fundamental principles of radiation protection when applied to the patient in diagnostic radiology. Radiat Prot Dosim. 2017;175:1–9.
44. Moores BM. The psychology of decision making and its relevance to radiation protection of the patient in medicine. Radiat Prot Dosim. 2018;178:245–53.
45. Moores BM, Stieve FE, Eriskat H, Schibilla H, editors. Technical and physical parameters for quality assurance in medical diagnostic radiology. British Institute of Radiology, BIR report 18; 1989.
46. Moores BM, Wall BF, Eriskat H, Schibilla H, editors. Optimization of image quality and patient exposure in diagnostic radiology. British Institute of Radiology, BIR report 20; 1989.
47. National Council on Radiation Protection and Measurements. Permissible dose from external sources of ionizing radiation. NRCP report no. 17; 1954.
48. National Council on Radiation Protection and Measurements. Ionizing radiation exposure of the population of the United States. NRCP report no. 160; 2009.
49. Oestreich AE. ALARA 1912: “as low a dose as possible” a century ago. Radiographics. 2014;34:1457–60.
50. Oikarinen H, Meriläinen S, Pääkkö E, Karttunen A, Nieminen MT, Tervonen O. Unjustified CT examinations in young patients. Eur Radiol. 2009;19:1161–5.
51. Parliament of the United Kingdom. Health and safety at work etc act. UK; 1974.
52. Pearce MS, Salotti JA, Little MP, McHugh K, Lee C, Kim KP, Howe NL, Ronckers CM, Rajaraman P, Craft AW, Parker L, Berrington de González A. Radiation exposure from CT scans in childhood and subsequent risk of leukaemia and brain tumours: a retrospective cohort study. Lancet. 2012;380:499–505.
53. Perlmutter N, Arthur RJ, Beluffi G, Cook V, Horwitz EA, Kramer P, Montagne JP, Thomas PS, Schneider K. The quality criteria for diagnostic radiographic images in paediatrics. Radiat Prot Dosim. 1998;80:45–8.
54. Portelli JL, McNulty JP, Bezzina P, Rainford L. Frequency of paediatric medical imaging examinations performed at a European teaching hospital over a 7-year period. Eur Radiol. 2016;26:4221–30.
55. Pouders E, Van Tiggelen R. Milestones in paediatric radiology. JBR-BRT. 2007;90:15–7.
56. Regulla D, Eder H. Patient exposure in medical x-ray imaging in Europe. Radiat Prot Dosim. 2005;114:11–25.
57. Reyher P. Das Röntgenverfahren in der Kinderheilkunde. Berlin: Hermann Meusser; 1912.
58. Röntgen WC. Ueber eine neue Art von Strahlen. (Vorläufige Mittheilung.) Sitzungsberichte der Würzburger Physik. medic. Gesellschaft. 1895:137–47.
59. Rotch TM. Living anatomy and pathology; the diagnosis of diseases in early life by the Roentgen method. Philadelphia, London: Lippincott Company; 1910.
60. Schegerer A. Diagnostische Referenzwerte für diagnostische und interventionelle Röntgenanwendungen. Salzgitter: Bundesamt für Strahlenschutz; 2016.

61. Schneider K. Evolution of quality assurance in paediatric radiology. Radiat Prot Dosim. 1995;57:119–23.
62. Seidenbusch MC, Schneider K. Radiation exposure of children in pediatric radiology. Part 1: referral criteria and x-ray examination frequencies at a university children's hospital between 1976 and 2003. Fortschr Röntgenstr. 2008;180:410–22.
63. Seidenbusch MC, Schneider K. Strahlenhygienische Aspekte bei der Röntgenuntersuchung des Thorax. Radiologe. 2015;55:580–7.
64. Stephan G, Schneider K, Panzer W, Walsh L, Oestreicher U. Enhanced yield of chromosome aberrations after CT examinations in paediatric patients. Int J Radiat Biol. 2007;83:281–7.
65. Unites Nations. Convention of the rights of the child; 1989.
66. United Nations Scientific Committee on the Effects of Atomic Radiation (UNSCEAR). UNSCEAR 2013 Report, Volume II: scientific findings on effects of radiation exposure of children, Scientific Annex B: effects of radiation exposure of children. ISBN 978-92-1-142293-1, New York: United Nations; 2013.
67. Willich E, Ebel KD. The history of paediatric radiology in Germany. In: Kaufmann HJ, Ringertz H, Sweet E, editors. The first 30 years of the ESPR. Berlin, Heidelberg: Springer; 1995.
68. Willis CE, Slovis TL. The ALARA concept in pediatric CR and DR: dose reduction in pediatric radiographic exams—a white paper conference executive summary. Radiology. 2005;234:343–4.

2 The Concept of Normalized Organ Doses for Dose Reconstruction in Paediatric Radiology

2.1 Normalized Organ Doses

The estimation of the radiation exposure of the patient during X-ray examinations is an essential requirement in order to assess the stochastic radiation risk of the patient. In Chap. 3, an outline of the fundamentals of paediatric dosimetry will be given.

In recent years, the estimation of the organ doses received during conventional radiographic X-ray examinations has been usually performed by applying normalized organ doses (synonymously: conversion factors, conversion coefficients) to basic dose indicators like the incident air kerma or the dose area product which can be measured. This concept of normalized organ doses is highly applicable in clinical radiology as normalized organ doses for conventional radiographs are given in numerous individual publications and in a few large systematic reference tables which have been published in recent years (see Chap. 29). Thus, organ doses can be estimated easily and quickly from basic dose indicators like the incidence air kerma or the dose area product.

2.2 Normalized Organ Doses Considering Varying Field Settings

In the reference tables published up to now, the selection of exposure parameters and standardized radiation field settings (size and position of the radiation field on the patient) has been performed through the institutions publishing the reference tables of normalized organ doses. However, exposure parameters and radiation field settings applied in clinical practice may differ from the standard values given in the reference tables. Beyond that, the cited reference tables are lacking quantitative information regarding the impact of the variation of exposure parameters and field settings on the radiation exposure especially in such organs and tissues which are localized close to the radiation field. Thus, the normalized organ doses listed in these tables are probably not generally applicable to a particular clinical examination situation, or are only applicable with limitations.

For this reason in particular and for considering the varying radiation field settings in clinical routine, new sets of normalized organ doses for calculating organ doses from measured incidence doses have been provided by the authors of this book in recent years, basing on optimal and suboptimal radiation field settings and considering different age groups of 0,[1] 1, 5, 10, 15, and 30 years for the most frequent X-ray examinations, i.e. the skull, the thorax, the abdomen, the segmental spine, the

[1]The age group "0" refers to children having an age less than 1 year. Although this term can be criticized from the paediatric point of view, it is very appropriate for mathematically describing anthropometric properties.

M. Seidenbusch et al., *Imaging Practice and Radiation Protection in Pediatric Radiology*,
https://doi.org/10.1007/978-3-030-18504-6_2

pelvis, and the thoraco-abdominal radiograph in neonates and young infants [1–6].

However, due to the limited space available in scientific publications, only a small set of exposure parameters and field settings could be considered in these publications. As normalized organ doses are significantly affected by the radiation quality, the normalized organ doses listed in these publications may be not complete enough for any kind of clinical application. In addition, no standard operating procedures regarding the patient preparation, the field setting, and the exposure parameters depending on the patient's age could be provided. As the field setting and the exposure parameters do have strong impact on the organ doses achieved in a patient, an integrated presentation of clinical and dosimetric aspects seems to be essential in order to achieve a maximum of clinical applicability.

Therefore, the intention of this book has been to provide new normalized organ doses for all common conventional paediatric X-ray examinations in paediatric patients of all age groups considering various aspects of field setting, exposure parameters, image quality requirements, and radiation doses.

References

1. Seidenbusch MC, Regulla D, Schneider K. Radiation exposure of children in pediatric radiology. Part 2: the PAEDOS algorithm for computer-assisted dose reconstruction in pediatric radiology and results for x-ray examinations of the skull. Fortschr Röntgenstr. 2008;180:522–39.
2. Seidenbusch MC, Regulla D, Schneider K. Radiation exposure of children in pediatric radiology. Part 3: conversion coefficients for reconstruction of organ doses achieved during chest x-ray examinations. Fortschr Röntgenstr. 2008;180:1061–81.
3. Seidenbusch MC, Regulla D, Schneider K. Radiation exposure of children in pediatric radiology. Part 6: conversion coefficients for reconstruction of organ dose in abdominal radiography. Fortschr Röntgenstr. 2009;181:945–61.
4. Seidenbusch MC, Regulla D, Schneider K. Radiation exposure of children in pediatric radiology. Part 7: conversion factors for reconstruction of organ dose during thoracoabdominal babygrams. Fortschr Röntgenstr. 2010;182:415–21.
5. Seidenbusch MC, Schneider K. Conversion coefficients for determining organ doses in paediatric spine radiography. Pediatr Radiol. 2014;44:434–56.
6. Seidenbusch MC, Schneider K. Conversion coefficients for determining organ doses in paediatric pelvis and hip joint radiography. Pediatr Radiol. 2014;44:1110–23.

Part II

Fundamentals of Radiation Dosimetry in Conventional Paediatric Radiology

*"*Αεὶ ὁ ***θεὸς γεωμετρεῖ.*****"***—"God is ever doing geometry."*

Platon

3 Specific Problems of Paediatric Radiology

Children are not to be considered as "little adults" [10, 20, 93]. Thus, medical examinations in children will have to be different from those in adults [19]. This is particularly true for paediatric X-ray examinations [10]. Children differ from adults regarding

- anthropometry
- anatomy and physiology
- psychology
- radiation biology
- radiation risk

3.1 Anthropometry

"Anthropometry is the measurement of human size, shape, and physical capabilities" [37]. Anthropometry is as old as humanity.[1] In ancient Egypt and Greece, it was a common matter in knowledge of artists and philosophers that there inevitably had to exist a divine relationship between anthropometry and geometry. Probably one of the first of the ancient artists who described the divine proportions in humans was *Polyklet* [24, 56]. Once again in the Renaissance, artists like *Leonardo da Vinci* tried to find a relationship between human body measures and geometrical figures [13]. Across the millennia, there have been a lot of motivations for the geometric approach to human anthropometry: theology [13], natural philosophy [47], visual arts [13, 24, 39, 44, 56, 79, 86], architecture and ergonomics [15, 74], and last but not least medicine [1, 3, 6, 7, 22, 23, 29, 33, 36, 40, 41, 42, 46, 51, 54, 82, 85, 89, 92]. Indeed, anthropometry is an important measure in paediatrics e.g. for diagnosing disorders in the somatic evolution of children [3, 22, 36, 85]. But also in paediatric radiology, the anthropometry of children does play a crucial role as radiation exposure during conventional radiographs is an exponential function of patient diameter (see Chap. 4.6) [1, 29, 38, 40, 41, 42, 46] and thus has to be considered when planning paediatric CT protocols [55]. Beyond that, the effects of scatter radiation, collimation, and shielding are strongly affected by the children's body measures as well. As children's anthropometry does vary over a wide range not only during ontogenesis but also within a defined age group [e.g. [54, 85]], determining exposure parameters for performing paediatric X-ray examinations or reconstructing radiation doses achieved during X-ray examinations in children is rather extensive.

There are various publications about paediatric anthropometry. Modern relations between human's age and anthropometry have been established e.g. by various authors in the seventeenth century [39], in the eighteenth century [47], in the nineteenth century [63, 78], and in the twentieth century [3, 22, 54, 86, 92]. These findings

[1] During the national-socialistic period in Germany (1933–1945), anthropometry was misused for racist purposes. The German authors of this book distance themselves strongly from this approach.

M. Seidenbusch et al., *Imaging Practice and Radiation Protection in Pediatric Radiology*,
https://doi.org/10.1007/978-3-030-18504-6_3

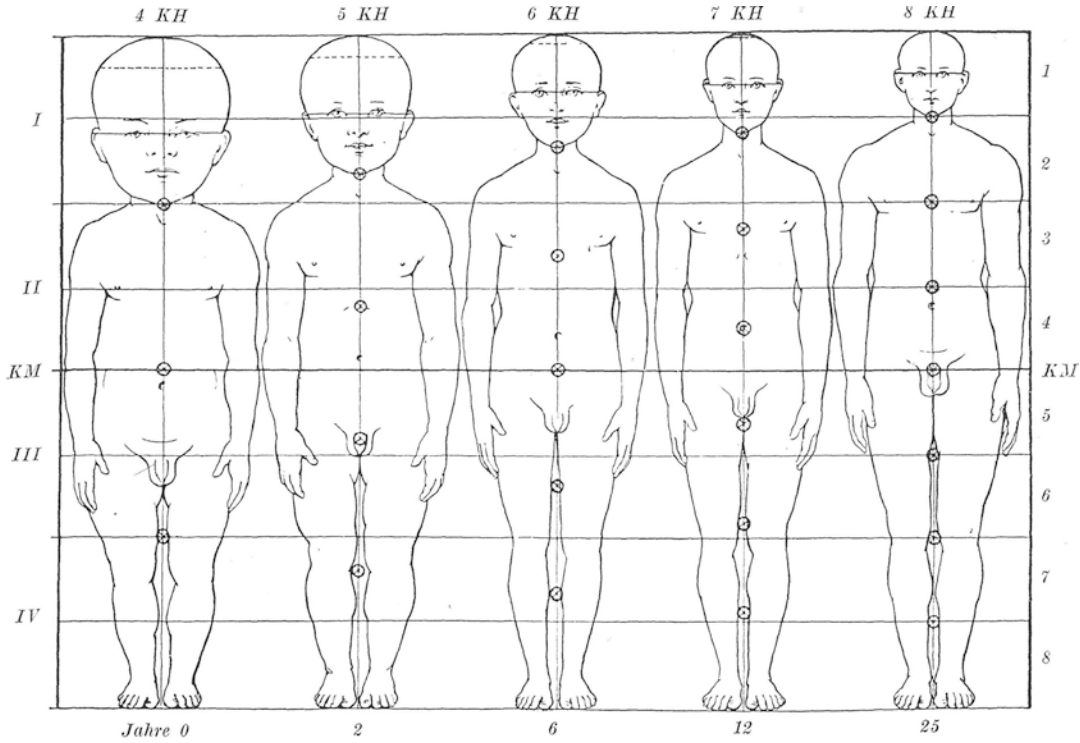

Fig. 3.1 Variation of human anthropometry over the years of life. Body measures are given in units of skull heights (KH = Kopfhöhe (German) = skull height, KM = Körpermittelpunkt (German) = midpoint of the body in the longitudinal axis) (From [54])

have also been transferred in textbooks of graphic art[2] [44, 86].

3.1.1 Body Height in Units of Head Heights

Figure 3.1 [54] shows the variation of human body measures as a function of age with the head height as measuring unit as it is common in visual arts [79] and probably was used first by *Polyklet* and his predecessors in ancient Greece and Egypt. A simple equation[3] can be used to describe the patient's total body height h_{Body} as a linear function of patient's age a in years (0–18 years) in terms of patient's head height h_{Head}:

$$h_{\text{Body}} = \left(\frac{2}{9}\cdot a + 4\right)\cdot h_{\text{Head}} \qquad (3.1)$$

3.1.2 Anthropometric Parameters of Anatomical Regions

Detailed anthropometric parameters of children are given in various publications, e.g. in the tables of *Bohmann* [6, 7] and Hart et al. [29]. More data have been provided e g. by *Snyder et al*. [74] and by the National Health and Nutrition Examination Surveys (NHANES) database [34]. In recent years, especially diameters of anatomical regions have been determined through several clinical studies. Numerical values of diameters of various anatomical regions being examined in paediatric patients are given also in the publications mentioned above [6, 7, 29, 36]. In many X-ray examinations, however, the trunk diameter of children does play a crucial role. As the human trunk region has an elliptical cylindrical shape, the

[2]It seems to be somewhat strange that data of human body proportions can be taken from textbooks of graphic art rather than from books of human anatomy, but indeed, anthropometry seems to be more a topic of visual arts and architecture than a topic of human medicine [49].

[3]This equation has been derived by the British painter *Martin Dace.*

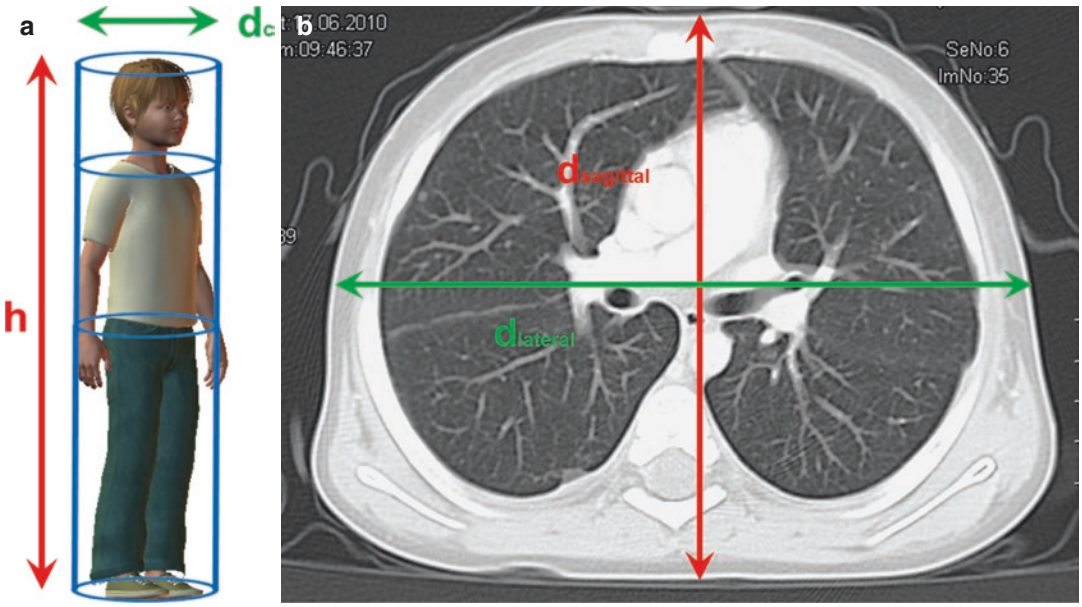

Fig. 3.2 Diameters of the trunk. (**a**) Concept of Lindskoug's equivalent cylindrical diameter. The equivalent diameter of the chest according to Lindskoug is derived from the patient's height h and the patient's mass m assuming the patient's body as a cylinder. The body density is assumed to be constant in all body regions. This approximation of the body of a paediatric patient by a cylinder is valid for children in their first 2 years of life. (**b**) Concept of the effective elliptical diameter. The effective elliptical diameter is the geometric mean of the sagittal and the lateral trunk diameter of the patient. Using computed tomography the diameters can be exactly measured [52, 64, 67]. (**b**) shows a chest CT image of a 6-month-old infant (© M. Seidenbusch 2018)

thickness of the human trunk can be described by its anatomical sagittal and lateral diameters d_{sagittal} and d_{lateral}.[4] For dosimetric purposes, it can be advantageous to calculate a virtual mathematical diameter representing these both real anatomical diameters.

Beyond that, also the chemical composition of organs and tissues determines the dosimetric properties of patients. Detailed chemical compositions are listed e.g. in [31].

3.1.3 Anthropometric Parameters of the Trunk Region

3.1.3.1 Equivalent Cylindrical Diameter of the Trunk Region

An approach to calculate a mathematical diameter from clinical anthropometric parameters is *Lindskoug's* concept of the equivalent cylindric diameter (in short: equivalent diameter) d_c (Fig. 3.2) [40, 41, 42, 46] which can be calculated from the patient's height h and mass m approximating the patient's shape by a cyclic cylinder with height h, diameter d_c, and medium density ρ:

$$d_c = \frac{2}{\sqrt{\pi \cdot \rho}} \cdot \sqrt{\frac{m}{h}} \tag{3.2}$$

3.1.3.2 Effective Elliptical Diameter of the Trunk Region

Another approach is the calculation of an effective elliptical diameter (in short: effective diameter) d_e from the real sagittal diameter d_{sagittal} and lateral diameter d_{lateral} considering the fact that the transversal section of human body has an elliptical shape [1, 9]:

$$d_e = \sqrt{d_{\text{sagittal}} \cdot d_{\text{lateral}}} \tag{3.3}$$

As can be seen e.g. in Chap. 4 from Table 4.3, the equivalent cylindrical diameter is closer to the

[4] By the way, during the adolescence, the ratio of the lateral to the sagittal diameter converges to the golden section [72].

sagittal diameter and the effective elliptical diameter is closer to the lateral diameter.

3.1.4 Anthropometric Parameters of the Skull

The anthropometric parameters of the skull (sagittal diameter, lateral diameter, head circumference, skull surface, brain weight, brain volume and many more) have been described since several centuries in numerous publications [e.g. [30, 54, 65, 89]]. In order to perform correct dosimetric calculations in paediatric patients, a realistic model of skull and brain are necessary especially in neonates and young infants because of the short distance between skull and trunk. Only then, scattered radiation originating from skull and chest is appropriately taken into account. In Chap. 4 will be shown that the skull volume has been considerably underestimated in the mathematical phantoms used for calculating the normalized organ doses in this book.

3.1.5 Somatograms

In paediatrics, for describing the age-related development of children, so-called somatograms are used which depict the dependence of body height ad body weight as functions of age [23, 51, 85]. As can be seen from somatograms derived from patients' anthropometric data acquired in the Dr. von Hauner Children's Hospital of the University of Munich during 1976–1998 [68], anthropometric properties such as body height and body weight show a wide range even within a defined age group (Figs. 3.3 and 3.4).

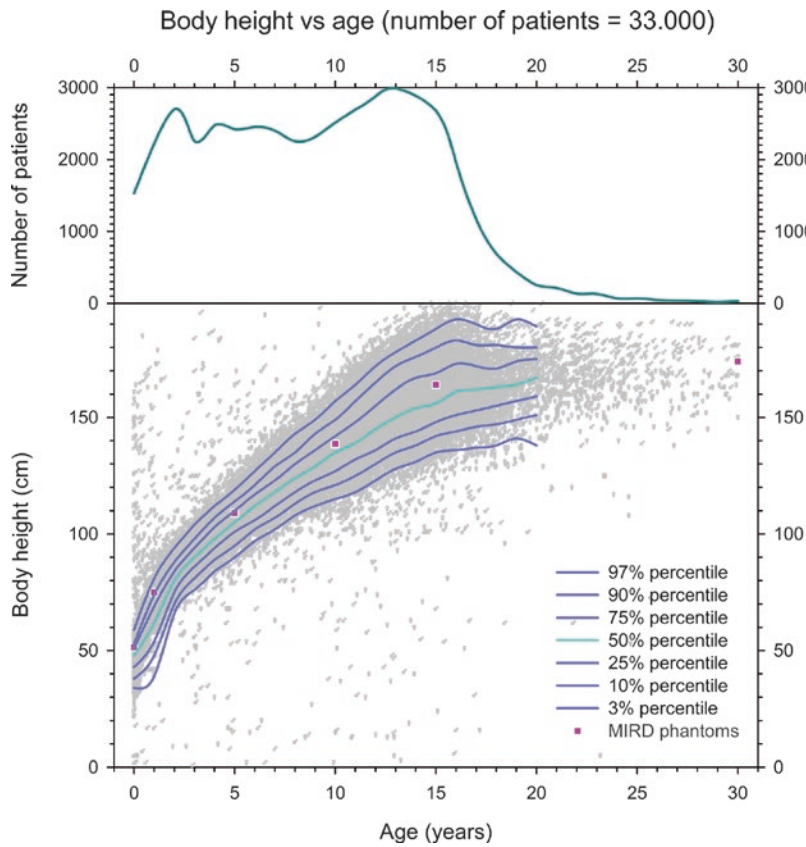

Fig. 3.3 Somatogram for body height of children in the Dr. von Hauner Children's Hospital, University of Munich, 1976–1998 [68]. Blue lines = 3%, 10%, 25%, 75%, 90%, and 97% percentiles; green line = 50% percentile = median; red squares = body heights of mathematical STUK MIRD phantoms. Body heights of STUK MIRD phantoms do match very well with the median body heights of the patient collective. The symbols represent original, uncorrected values as taken from the database of the paediatric radiology department (© M. Seidenbusch 2003)

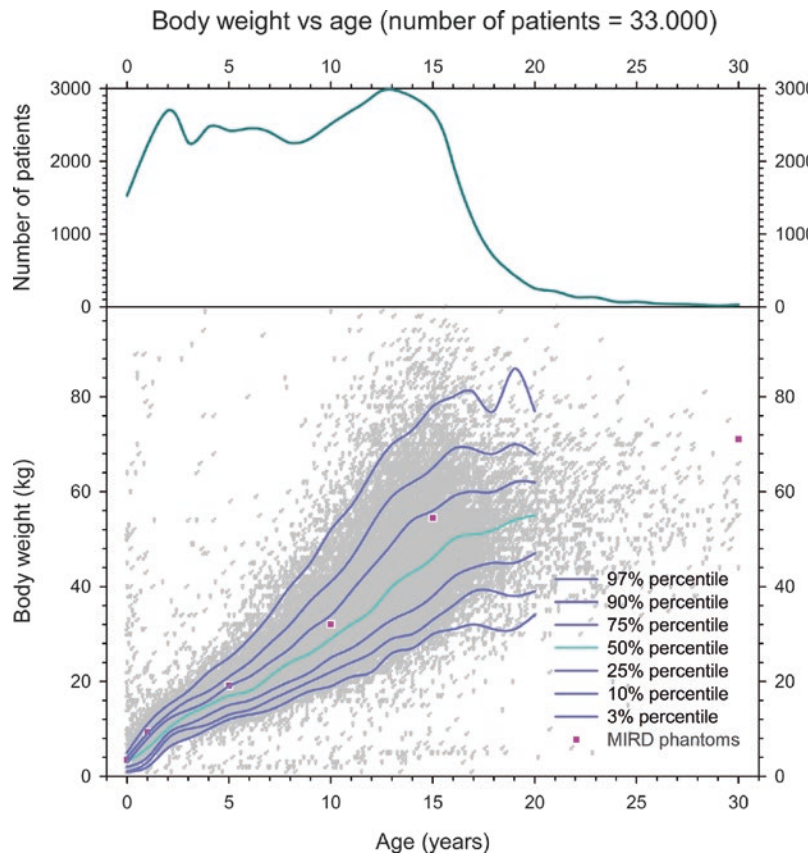

Fig. 3.4 Somatogram for body weight of children in the Dr. von Hauner Children's Hospital, University of Munich, 1976–1998 [68]. Blue lines = 3%, 10%, 25%, 75%, 90%, and 97% percentiles; green line = 50% percentile = median; red squares = body weights of mathematical STUK MIRD phantoms. Body weights of STUK MIRD phantoms do match very well with the median body weights of the patient collective. The symbols represent original, uncorrected values as taken from the database of the of the paediatric radiology department (© M. Seidenbusch 2003)

3.1.6 Age Groups[5]

The simplest way to assign normalized organ doses to a paediatric patient is characterizing the patient's anthropometry by his age. However, despite of the fact that patients' anthropometries may vary over a wide range even in the same age group, the definition of age groups may be reasonable not only for practical reasons.

There are various possibilities to define age groups for children [82]. From the medical point of view, the so-called traditional age groups can be defined (Table 3.1, [83]). Beyond that, according to numerous anthropometric considerations, several systems of age group intervals have been proposed (Table 3.2, [82]).

[5]The age group "0" refers to children having an age less than 1 year. Although this term can be criticized from the paediatric point of view, it is very appropriate for mathematically describing anthropometric properties.

Table 3.1 Traditional age groups [83]

Age group	Age range
Newborn	0–3 months
Infant	0–12 months
Toddler	–3 years
Preschool	–6 years
School age	–12 years
Adolescent	–18 years

Table 3.2 Examples for different age group systems [82]

Age group interval (years)				
Various countries [14, 26, 29, 47]	UK [32, 71, 72]	Japan [28]	Portugal [52]	Australia [7]
–	–	–	0–0.25	–
0–1	<1	<1	0.25–3	0–4
1–5	5	1–7	3–8	
5–10	10	8–12	8–15	5–14
10–15	–	13–19	15–19	–
–	–	>19	–	–

These age group intervals can be assigned to body weight intervals (Table 3.3, [84]).

Another approach is calculating age groups by defining equidistant trunk or body height intervals which can be derived from the anthropometric data published in somatograms (Tables 3.4 and 3.5 [83]).

In another approach, age group intervals are chosen in a way that within an age group organ sizes do not vary more than 15% (Table 3.6, [83]).

Overall, it can be stated that the age groups and age group intervals defined in Table 3.6 correspond to minimal variations of trunk or body height and of organ dimensions within an age group.

Table 3.3 Age groups corresponding to body weight intervals [84]

Age group interval (years)	Body weight interval (kg)
0–1	<10
1–5	10–20
5–10	20–35
10–15	>35

Table 3.4 Age groups corresponding to nearly equal trunk height intervals [83]

Age group (years)	Age range (years)	Trunk height range (cm)
0	0–0.5	10–24
1	0.5–3	24–30
5	3–7.5	30–36
10	7.5–12.5	36–42
15	12.5–17	42–50

Considering the medium percentile of a somatogram of trunk height vs. age, age ranges were derived from somatogram values corresponding to trunk height intervals between the age groups of about 6 cm

Table 3.5 Age groups corresponding to body height intervals [83]

Age group (years)	Age range (years)	Height range (cm)
0	0–0.5	0–66
1	0.5–3	66–95
5	3–7	95–124
10	7–13	124–156
15	13–17	156–168

Considering the medium percentile of a somatogram of body height vs. age, age ranges were derived from somatogram values corresponding to body height intervals of about 30 cm

Table 3.6 Age groups corresponding to variation of organ dimensions [83]

Age group (years)	Age range
0	0–0.5
1	0.5–3
5	3–7
10	7–13
15	13–17

Age groups are chosen in a way that within an age group organ sizes do not vary more than 15%

3.2 Anatomy and Physiology

Children differ from adults not only in anthropometry [33] but also in anatomy and physiology [54]. There are several implications arising from these differences: The age-depending anatomical situs of organs, the size of organs and tissues have an impact on X-ray findings. As in infants and young children organs are localized closer together than in older children, radiation protection through collimation or shielding is much more sophisticated. Beyond that, the age-related specific peculiarities of the physiology, e.g. respiratory rate, have to be considered. By this means, the exposure time should be as low as possible in uncooperative patients. It should be kept below 4 ms for ap chest X-rays in infants to avoid motion and minimize pulsation artefacts of small intrapulmonary interstitial pulmonary structures [10]. In this paragraph, reference will be made to some age-specific properties of some organs and tissues insofar they are important for radiation protection. The following paragraphs refer also to the STUK MIRD phantom family described in Chap. 4.8.

3.2.1 Skull

The ocular lenses are not inserted in the STUK-phantoms. Therefore, no calculations of the lens dose are possible.

In first year of life, a considerable proportion of the active bone marrow (about 30%) is located in the cranial vault and the facial bones. This proportion of bone marrow decreases continuously over the years. Post puberty it is in the range of 10% of the total.

3.2.2 Thymus

The thymus varies greatly in size and shape up to the age of 2 years. The cervical lobe of the thymus—a frequent anomaly in infancy—is not incorporated in the STUK MIRD phantoms. This variant underestimates the thymus dose even if the skull ap radiograph is collimated tightly (optimal field setting).

3.2.3 Chest

Size and shape of the human chest depend on patient's age [6, 7, 61, 72]. Thus, the sagittal and lateral chest diameters are a function of age. In elder children, the increase of the lateral chest diameter has been overestimated when the phantom family of PCXMC program was created [72].

3.2.4 Lungs

The lung density and thus the value of the effective linear mass-attenuation coefficients (see Chap. 4) of the lungs decrease with patient's age [35, 43, 72, 77]. This can be explained by the enlargement of the air spaces with simultaneous decrease of the interstitial tissue of the developing lungs. This process, the continuing increase in number and size of the alveoli occurs within the first 7 years of life. At the same time, the patient's diameters grow preferably in the horizontal and longitudinal direction with age. These two characteristics implicate that the radiation doses required for chest radiographs can be kept nearly constant over the age range from infants till the age of 10 years, a physical effect which at first glance may seem somewhat strange but which is well known in clinical routine [71].

3.2.5 Mammae

Post-partum maternal hormones can sensitize the breast tissue of full-term newborns leading to a transient increase of the mammary tissue. This increase of glandular tissue mass in the first 3–6 months of life has not been respected when the phantom family of PCXMC program was created [69]. The glandular breast tissue in this age period is probably more vulnerable to ionizing radiation as the mitotic activity is increased [90].

3.2.6 Gonads

The location of ovaries varies considerably in all age groups of females. In neonates they are often located higher in the pelvic region than in older girls or adolescents. One reason for the high position is a long mesovar which allows the ascension of ovaries even into the upper abdomen [2, 14, 18, 21, 58]. The size of the urinary bladder can also change the position of the ovaries considerably.

The male gonads descend to the scrotum. This process is not finished before the school age. In premature male babies born before the 28th gestational week, they are located within the abdomen.

3.2.7 Active Bone Marrow

The active bone marrow with its stem cells is amongst the most radiation-sensitive tissues in human body. Therefore, the radiation exposure of active bone marrow will contribute significantly to the total stochastic radiation risk. The estimation of the active bone marrow dose requires detailed quantitative information about its regional distribution in the different compartments of the human body. This regional distribution of red bone marrow cells, however, is depending on age [11, 16, 62, 66, 87, 88, 91]. For example, in premature babies with a gestational age of 28 weeks, erythropoietic stem cells are mainly found in the liver with a percentage of 50% and in the spleen with a percentage of 15% [50]. Even in mature neonates, during the first weeks of life, not all stem cells will have migrated to the active bone marrow. It must be stated here that it remains questionable whether these aspects have been considered sufficiently when constructing the mathematical MIRD phantoms

forming the basis of the normalized organ doses listed in this book.

As active bone marrow cells are enclosed by bone cells and as the linear mass absorption coefficients (see Chap. 4) of bone are higher than these of red bone marrow, interface effects may play an important role during radiation exposure of active bone marrow cells [75] resulting in a local dose enhancement which likely cannot be calculated through the conventional phantom models used in radiation dosimetry.

3.3 Psychology

It may be somewhat surprising at first glance that even children's psychology should play an important role in paediatric radiology [5, 80]. However, already in 1911, the German paediatrician *Reyher* reported that X-ray examinations create additional distress for the child [60]. Indeed, for a child, "admission to hospital is a kind of trap from which there is no escape" [20], and "there is always the fear of unknown" [20]. Moreover, "large [X-ray] machines are intimidating, and most children do not like the feeling that they are trapped under something which may fall on them" [20]. Therefore, children often will not cooperate during medical examinations or even try to escape, especially during X-ray examinations. Of course, a restless child will enhance the number of motion artefacts during X-ray examinations [59]. Thus, from the dosimetric point of view, this behaviour of children may result in repeated radiographs or in extended fluoroscopy durations. As a consequence, the radiation burden in uncooperative children may be increased compared to the radiation doses achieved in cooperating children.[6,7]

[6]Moreover, also the parents' psychology may be taken into consideration as the perception of radiation risk is rather different in different population groups [17, 45] and thus affects radiation risk communication in clinical practice.

[7]More literature about this subject has been provided in [80].

3.4 Radiation Biology

As mentioned in the Introduction section, children have to be considered as being much more radiation-sensitive than adults. The radiation exposure in children under 10 years has been assumed to increase the stochastic radiation risk by a factor of 3–4 [32]. Radio-biological investigations have shown in recent years that at least some organs and tissues in children seem to be much more sensitive to ionizing radiation than those of adults [76, 81]. In particular, children younger than 10 years seem to be more radiation-sensitive than adolescents. Finally, this factor may be of wider importance as a lot of paediatric X-ray examinations are performed in neonates and young infants [70, 73]. The reason for the enhanced radiosensitivity of children may be the fact "that radiosensitivity of tissues depends upon the number of undifferentiated cells which the tissue contains, the degree of mitotic activity in the tissue, and the length of time that the cells of the tissue stay in active proliferation" (law of *Bergonié* and *Tribondeau*) [4, 57] and all of these factors are enhanced in children.

3.5 Radiation Risk

Against this background, the question comes up whether children have an increased stochastic radiation risk through paediatric X-ray examinations. For the dose range of conventional X-ray examinations, no significant enhancement of stochastic radiation risk could be found in epidemiologic studies [e.g. [25–28]]. However, *Brenner et al.* assumed that the stochastic radiation risk of children might be considerably increased by paediatric CT examinations [8]. According to this, direct epidemiologic proof of a significantly heightened risk for neoplastic diseases after CT examinations in the age range under 22 years has been given [48, 53].

References

1. American Association of Physicists in Medicine. Size-specific dose estimates (SSDE) in pediatric and adult body CT examinations. AAPM report 204; 2011.
2. Bardo DME, Black M, Schenk K, Zaritzky MF. Location of the ovaries in girls from newborn to 18 years of age: reconsidering ovarian shielding. Pediatr Radiol. 2009;39:253–9.
3. Bakwin H, Bakwin RM. Body build in infants: V. Anthropometry in the new-born. Human Biol. 1934;6:612–26.
4. Bergonié J, Tribondeau L. Interprétation de quelques résultats de la radiothérapie et essai de fixation d'une technique rationnelle. C R Acad Sci. 1906;143:983–5.
5. Björkman B. Children in the radiology department—a study of anxiety, pain, distress and verbal interaction. Thesis, Jönköping University, Dissertation series no. 51; 2014.
6. Bohmann I. Ermittlung des Durchstrahlungsdurchmessers bei Säuglingen, Kindern und Jugendlichen zur Aufstellung von Belichtungswerten in der Röntgendiagnostik und Abschätzung der Organdosiswerte bei typischen Röntgenuntersuchungen. Dissertation, Universität München; 1990.
7. Bohmann I. Ermittlung des Durchstrahlungsdurchmessers bei Säuglingen, Kindern und Jugendlichen zur Aufstellung von Belichtungswerten in der Röntgendiagnostik und Abschätzung der Organdosiswerte bei typischen Röntgenuntersuchungen. GSF-Bericht 16/90; 1990.
8. Brenner DJ, Elliston CD, Hall EJ, Berdon WE. Estimated risks of radiation-induced fatal cancer from pediatric CT. AJR. 2001;176:289–96.
9. Burton CS, Szczykutowicz TP. Evaluation of AAPM reports 204 and 220: estimation of effective diameter, water-equivalent diameter, and ellipticity ratios for chest, abdomen, pelvis, and head CT scans. J Appl Clin Med Phys. 2018;19:228–38.
10. Commission of the European Communities. European guidelines on quality criteria for diagnostic radiographic images in paediatrics. EUR 16261, SBN 92-827-7843-6; 1996.
11. Cristy M. Active bone marrow distribution as a function of age in humans. Phys Med Biol. 1981;26:389–400.
12. Daldrup-Link HE, Gooding CA, editors. Essentials of pediatric radiology. New York: Cambridge University Press; 2010.
13. Da Vinci L. In: Pacioli L, editor. De divina proportione. Venice: Paganini; 1509.
14. Dawood RM, Hall CM. Too much radiation for too many children? Br Med J. 1988;296:1277–8.
15. Dreyfuss H. The measure of man. Human factors in design. New York: Whitney Library of Design; 1967.
16. Ellis RE. The distribution of active bone marrow in the adult. Phys Med Biol. 1961;5:255–8.
17. European Commission. Radiation protection No 184—EU Scientific Seminar 2015 "Risk communication". Directorate-General for Energy, Directorate D—Nuclear Energy, Safety and ITER, Unit D3—Radiation Protection and Nuclear Safety; 2016.
18. Featherstone C, Harnett AN, Brunt AM. Ultrasound localization of the ovaries for radiation-induced ovarian ablation. Clin Oncol. 1999;11:393–7.
19. Fendel H, Schneider K, Bakowski C, Glas J, Drews K, Kohn MM. The efficacy of diagnostic radiation in paediatrics. Report of the Federal Ministry for Environment, Environment Protection and Reactor Safety of the Federal Republic of Germany, BMU-1987-161; 1987.
20. Fendel H, Sweet EM, Thomas PS, editors. The status of paediatric radiology in Europe. Berlin: Schering AG; 1991. isbn:3-921817-43-9.
21. Fochem K, Pape R. Problematik des Ovarialschutzes bei Röntgenaufnahmen des Beckens. Fortschr Röntgenstr. 1962;97:785–79.
22. Friedenthal HWC. Allgemeine und spezielle Physiologie des Menschenwachstums. Berlin: Springer; 1914.
23. Fryar CD, Gu Q, Ogden CL. Anthropometric reference data for children and adults: United States, 2007–2010. National Center for Health Statistics. Vital Health Stat. 2012;(252):1–48.
24. Galenos of Pergamon A. De placitis Hippocratis et Platonis 5, 449.
25. Hammer GP, Seidenbusch MC, Regulla DF, Spix C, Zeeb H, Schneider K, Blettner M. Childhood cancer risk from conventional radiographic examinations for selected referral criteria: results from a large cohort study. AJR. 2011;197:217–23.
26. Hammer GP, Blettner M, Schneider K, Seidenbusch MC, Regulla DF. Kohortenstudie zur Abschätzung des Krebsrisikos durch diagnostische Strahlenexposition im Kindesalter (RICC-Studie). Ergebnisbericht, Forschungsvorhaben StSch 4432, Bundesamt für Strahlenschutz, urn:nbn:de:0221-2009011214, Salzgitter; 2009.
27. Hammer GP, Seidenbusch MC, Schneider K, Regulla DF, Zeeb H, Spix C, Blettner M. A cohort study of childhood cancer incidence after postnatal diagnostic x-ray exposure. Radiat Res. 2009;171:504–12.
28. Hammer GP, Seidenbusch MC, Schneider K, Regulla DF, Zeeb H, Spix C, Blettner M. Cancer incidence rate after diagnostic x-ray exposure in 1976–2003 among patients of a university children's hospital. Fortschr Röntgenstr. 2010;182:404–14.
29. Hart D, Wall BF, Shrimpton PC, Bungay DR, Dance DR. Reference doses and patient size in paediatric radiology. Didcot: National Radiological Protection Board NRPB-R318; 2000. isbn:0-85951-448-X.
30. Huschke E. Schaedel, Hirn und Seele des Menschen und der Thiere nach Alter, Geschlecht und Race, dargestellt nach neuen Methoden und Untersuchungen. Jena: Friedrich Mauke Verlag; 1854.
31. International Commission on Radiological Protection. Report of the task group on reference man: anatomi-

cal, physiological and metabolic characteristics. ICRP publication 23. Oxford: Pergamon Press; 1975.
32. International Commission on Radiological Protection. 1990 recommendations of the International Commission on Radiological Protection. ICRP publication 60. Oxford: Pergamon Press; 1990.
33. International Commission on Radiological Protection. Basic anatomical and physiological data for use in radiological protection: reference values. ICRP publication 89. Oxford: Pergamon Press; 2003.
34. Johnson PB, Whalen SR, Wayson M, Juneja B, Lee C, Bolch WE. Hybrid patient-dependent phantoms covering statistical distributions of body morphometry in the U.S. adult and pediatric population. Proc IEEE. 2009;97:2060–75.
35. Kalender WA, Rienmüller R, Seissler W, Behr J, Welke M, Fichte H. Measurement of pulmonary parenchymal attenuation: use of spirometric gating with quantitative CT. Radiology. 1990;175:265–8.
36. Kleinman PL, Strauss KJ, Zurakowski D, Buckley KS, Taylor GA. Patient size measured on CT images as a function of age at a tertiary care children's hospital. AJR. 2010;194:1611–9.
37. Klinich KD, Reed MP. Pediatric anthropometry. In: Crandall JR, Myers BS, Meaney DF, Zellers-Schmidtke S, editors. Pediatric injury biomechanics. New York: Springer company; 2013. p. 1–31.
38. Ladia AP, Skiadopoulos SG, Karahaliou AN, Messaris GAT, Delis HB, Panayiotakis GS. The effect of increased body mass index on patient dose in paediatric radiography. Eur J Radiol. 2016;85:1689–94.
39. Lautensack H. Dess Cirkelss und Richtscheyts, auch der Perspectiva, und Proportion der Menschen und Rosse. Simon Schamberger; 1618.
40. Lindskoug BA. The reference man in diagnostic radiology dosimetry. Br J Radiol. 1992;65:431–7.
41. Lindskoug BA. Reference man in diagnostic radiology dosimetry. Radiat Prot Dosim. 1992;43:111–4.
42. Lindskoug BA. Exposure parameters in x ray diagnostics of children, infants and the newborn. Radiat Prot Dosim. 1992;43:289–92.
43. Long FR, Williams RS, Castile RG. Inspiratory and expiratory CT lung density in infants and young children. Pediatr Radiol. 2005;35:677–83.
44. Loomis A. Figure drawing for all it's worth. London: Chapman & Halls; 1943.
45. Luetzelschwab J. The 3 R's: radiation, risk, and reason. Carlisle: Dickinson College, Department of Physics; 1996.
46. Martin CJ, Farquhar B, Stockdale E, Macdonald S. A study of the relationship between patient dose and size in paediatric radiology. Br J Radiol. 1994;67:864–71.
47. Martinet JF. Katechismus der natuur. Amsterdam: Joanne van Selm; 1777.
48. Mathews JD, Forsythe AV, Brady Z, Butler MW, Goergen SC, Byrnes GB, Giles GG, Wallace AB, Anderson PR, Guiver TA, McGale P, Cain TM, Dowty JG, Bickerstaffe AC, Darby SC. Cancer risk in 680 000 people exposed to computed tomography scans in childhood or adolescence: data linkage study of 11 million Australians. BMJ. 2013;346:f2360.
49. Milz S. Private communication. Chair of anatomy. Munich: University of Munich; 2018.
50. Nathan DG, Oski FA. Hematology of infancy and childhood, vol. I. Philadelphia: Holt-Saunders; 1981.
51. Neuhauser H, Schienkiewitz A, Schaffrath Rosario A, Dortschy R, Kurth BM. Referenzperzentile für anthropometrische Maßzahlen und Blutdruck aus der Studie zur Gesundheit von Kindern und Jugendlichen in Deutschland (KiGGS). Berlin: Robert Koch-Institut; 2013. isbn:978-3-89606-218-5.
52. Parikh RA, Wien MA, Novak RD, Jordan DW, Klahr P, Soriano S, Ciancibello L, Berlin SC. A comparison study of size-specific dose estimate calculation methods. Pediatr Radiol. 2018;48:56–65.
53. Pearce MS, Salotti JA, Little MP, McHugh K, Lee C, Kim KP, Howe NL, Ronckers CM, Rajaraman P, Craft AW, Parker L, Berrington de González A. Radiation exposure from CT scans in childhood and subsequent risk of leukaemia and brain tumours: a retrospective cohort study. Lancet. 2012;380:499–505.
54. Peter K, Wetzel G, Heiderich F, editors. Handbuch der Anatomie des Kindes. München: Verlag von J. F. Bergmann; 1938.
55. Phillips GS, Stanescu AL, Alessio AM. Relationships of pediatric anthropometrics for CT protocol selection. AJR. 2014;203:W85–91.
56. Philon of Byzanz. Mechanike syntaxis 4, 1, 49.
57. Pizzarello DJ, Witcofski RL. Basic radiation biology. Philadelphia: Lea & Febiger; 1967.
58. Poretti GG. Radiation exposure of a population due to diagnostic x-ray examinations: some critical remarks. Phys Med Biol. 1985;30:1017–27.
59. Poznanski EO. Some psychologic factors affecting the child in the radiology department. In: Poznanski AK, editor. Practical approaches to pediatric radiology. Chicago: Year Book Medical Publishers; 1976. p. 55–9.
60. Reyher P. Das Röntgenverfahren in der Kinderheilkunde. Berlin: Hermann Meusser; 1912.
61. Riccabona M, Beer M, Mentzel H-J, editors. Bildgebung des Thorax bei Neugeborenen und Kleinkindern. Berlin: Springer; 2019.
62. Ricci C, Cova M, Kang YIS, Yang A, Rahmouni A, Scott WW, Zerhouni EA. Normal age-related patterns of cellular and fatty bone marrow distribution in the axial skeleton: MR imaging study. Radiology. 1990;177:83–8.
63. Richer P. Description des formes extérieures du corps humain au repos et dans les principaux mouvements. Paris: Imprimeurs-éditeurs Plon, Nourrit et Cie; 1890.
64. Richter E, Lierse W. Radiologische Anatomie des Neugeborenen. Gesicht, Hals und Thorax. München: Urban & Schwarzenberg; 1990. p. 68–146.
65. Schienkiewitz A, Schaffrath Rosario A, Dortschy R, Ellert U, Neuhauser H. German head circumference references for infants, children and adolescents in comparison with currently used national and international references. Acta Paediatr. 2011;100:e28–33.
66. Schneider C, Montz R. Die quantitative Verteilung des erythropoetischen Knochenmarks beim Menschen gemessen mit Radioeisen. J Mol Med. 2005;16:969–73.

67. Schneider K. The normal child: growth and development of the infant and the child; frequent and important variants. In: Daldrup-Link HE, Gooding CA, editors. Essentials of pediatric radiology. New York: Cambridge University Press; 2010. p. 1–19.
68. Seidenbusch M. Rekonstruktion von Organ- und Effektivdosen bei konventionellen Röntgenuntersuchungen am Dr. von Haunerschen Kinderspital der Universität München mit einer Berechnung neuer Konversionsfaktoren für die pädiatrische Radiologie. Dissertation, LMU München: Medizinische Fakultät; 2006.
69. Seidenbusch M, Kammer B, Specht T, Stahl R, Schneider K. Zur Rekonstruktion der Brustdrüsendosis bei Kindern in der pädiatrischen Radiologie: Gewicht, Dichte und Volumen der Mammagewebe bei Neugeborenen, Säuglingen, Kleinkindern und Adoleszenten und die dosimetrischen Konsequenzen. Fortschr Röntgenstr. 2018;190:869–70.
70. Seidenbusch MC, Schneider K. Radiation exposure of children in pediatric radiology. Part 1: referral criteria and x-ray examination frequencies at a university children's hospital between 1976 and 2003. Fortschr Röntgenstr. 2008;180:410–22.
71. Seidenbusch MC, Schneider K. Radiation exposure of children in pediatric radiology. Part 4: entrance doses achieved during the x-ray examination of the chest. Fortschr Röntgenstr. 2008;180:1082–103.
72. Seidenbusch MC, Schneider K. Zur Strahlenexposition von Kindern in der pädiatrischen Radiologie. Anthropometrische Merkmale von Kindern und den zur Dosisrekonstruktion verwendeten mathematischen Phantomen (ISIMEP-Projekt des Bundesministeriums für Bildung und Forschung, Förderkennzeichen 02NUK016A). Fortschr Röntgenstr. 2012;184:A13.
73. Seidenbusch MC, Schneider K. Strahlenhygienische Aspekte bei der Röntgenuntersuchung des Thorax. Radiologe. 2015;55:580–7.
74. Snyder RG, Schneider LW, Owings CL, Reynolds HM, Golomb DH, Schork MA. Anthropometry of infants, children, and youths to age 18 for product safety design. Report UM-HSRI-77-17. Michigan: Highway Safety Research Institute, University of Michigan; 1977.
75. Spiers FW. Transition-zone dosimetry. Radiat Dosimetry. 1969;3:809–67.
76. Stephan G, Schneider K, Panzer W, Walsh L, Oestreicher U. Enhanced yield of chromosome aberrations after CT examinations in paediatric patients. Int J Radiat Biol. 2007;83:281–7.
77. Stein JM, Walkup LL, Brody AS, Fleck RJ, Woods JC. Quantitative CT characterization of pediatric lung development using routine clinical imaging. Pediatr Radiol. 2016;46:1804–12.
78. Stratz CH. Der Körper des Kindes und seine Pflege. Stuttgart: Enke Verlag; 1903.
79. Stratz CH. Die Darstellung des menschlichen Körpers in der Kunst. Berlin: Springer; 1914.
80. Thacker PG, Collins HR, Hill J. Distress experienced during pediatric VCUGs—a granular, prospective assessment using the brief behavioral distress scale. Pediatr Radiol. 2016;46:660–5.
81. United Nations Scientific Committee on the Effects of Atomic Radiation (UNSCEAR). UNSCEAR 2013 Report, Volume II: Scientific findings on effects of radiation exposure of children, Scientific Annex B: Effects of radiation exposure of children. ISBN 978-92-1-142293-1, United Nations, New York; 2013.
82. Vassileva J, Rehani M. Patient grouping for dose surveys and establishing diagnostic reference levels in paediatric computed tomography. Radiat Prot Dosimetry. 2015;65:81–5.
83. Varchena V. Pediatric phantoms. Pediatr Radiol. 2002;32:280–4.
84. Verdun F, Gutierrez D, Vader JP, Aroua A, Alamo-Maestre LT, Bochud F, Gudinchet F. CT radiation dose in children: a survey to establish age-based diagnostic reference levels in Switzerland. Eur Radiol. 2008;18:1980–6.
85. Voigt M, Fusch C, Olbertz O, Hartmann K, Rochow N, Renken C, Schneider KTM. Analysis of the neonatal collective in the Federal Republic of Germany. 12th report: presentation of detailed percentiles for the body measurement of newborns. Geburtsh Frauenheilk. 2006;66:956–70.
86. Von Froriep A. Anatomie für Künstler. Kurzgefasstes Lehrbuch der Anatomie, Mechanik, Mimik und Proportionslehre des menschlichen Körpers. Leipzig: Johann Ambrosius Barth Verlag; 1937.
87. Waitches G, Zawin JK, Poznanski AK. Sequence and rate of bone marrow conversion in the femora of children as seen on MR imaging: are accepted standards accurate? AJR. 1994;162:1399–406.
88. Wall BF, Shrimpton PC. Bone marrow dose in chest radiography: the posteroanterior vs. anteroposterior projection. Letter to the editor. Radiology. 1980;137:258–9.
89. Welcker H. Wachsthum und Bau des menschlichen Schädels. Leipzig: Wilhelm Engelmann Verlag; 1862.
90. Weninger WJ, Meng S, Geyer SH, Weninger SUG. Morphologie und funktionelle Anatomie des wachsenden Thorax. Radiologe. 2003;43:1036–44.
91. Wilpshaar J, Jokes EC, Lim FTH, van Leuwwen GHM, van den Boogaard PJ, Kanhai HHH, Willemze R, Falkenburg JHF. Magnetic resonance imaging of fetal bone marrow for quantitative definition of the human fetal stem cell compartment. Blood. 2002;100:451–7.
92. World Health Organization. WHO child growth standards. Length/height-for-age, weight-for-age, weight-for-length, weight-for-height and body mass index-for-age. Geneva: World Health Organization; 2006. isbn: 92 4 154693 X.
93. World Health Organization. WHO training package for the health sector, children's health and the environment: children are no little adults. Geneva: World Health Organization; 2008.

4 Radiation Dose and Dose Reconstruction in Conventional Paediatric Radiology

4.1 Introduction

Radiation dosimetry is the science of determining the fraction of the energy which is absorbed in matter during interaction with ionizing radiation [5]. Due to the fact that children are much more sensitive to ionizing radiation than adults, radiation dosimetry may be considered as one of the most important topics in paediatric radiology. In this chapter, the fundamentals of radiation dosimetry against the background of paediatric radiology will be presented. Therefore, the description of radiation physics will be focus on clinical paediatric aspects. For a more physical description, see e.g. [1, 5, 13, 17, 33, 40, 46].

Organ doses achieved in patients during conventional paediatric X-ray examinations depend on many influence parameters. Thus, radiation dosimetry and dose reconstruction are the most sophisticated subjects in paediatric radiology. In the following section, a short overview over the fundamentals of radiation dosimetry in paediatric radiology shall be given in order to enable the reader to perform dose reconstructions in children using this book. For more details in clinical radiation physics, see e.g. the books of *Bushberg* et al. [13] and *Dance* et al. [14].

4.2 Technical Principle of a Conventional X-Ray Examination

In order to achieve optimal image quality under optimized radiation exposure to the patient during an X-ray examination, the technical components of an X-ray unit and the physical exposure parameters have to be simultaneously adapted to each other with a lot of care. Figure 4.1 exemplifies the technical principle of a standard paediatric X-ray examination by a chest radiography in a 5-year-old patient and the exposure parameters associated to the technical components of the X-ray unit. From the technical point of view, a conventional X-ray examination works as follows.

4.2.1 X-Ray Tube

An electric field between the cathode and the anode is generated in the X-ray tube (depicted in Fig. 4.2) by connecting the cathode material with the negative pole and the anode material with the positive pole of a high voltage source with voltage V. Electrons with elementary electric charge e are released from a glow filament connected with the cathode and are accelerated in the electric field up to a kinetic energy E_{kin} when hitting the anode:

M. Seidenbusch et al., *Imaging Practice and Radiation Protection in Pediatric Radiology*,
https://doi.org/10.1007/978-3-030-18504-6_4

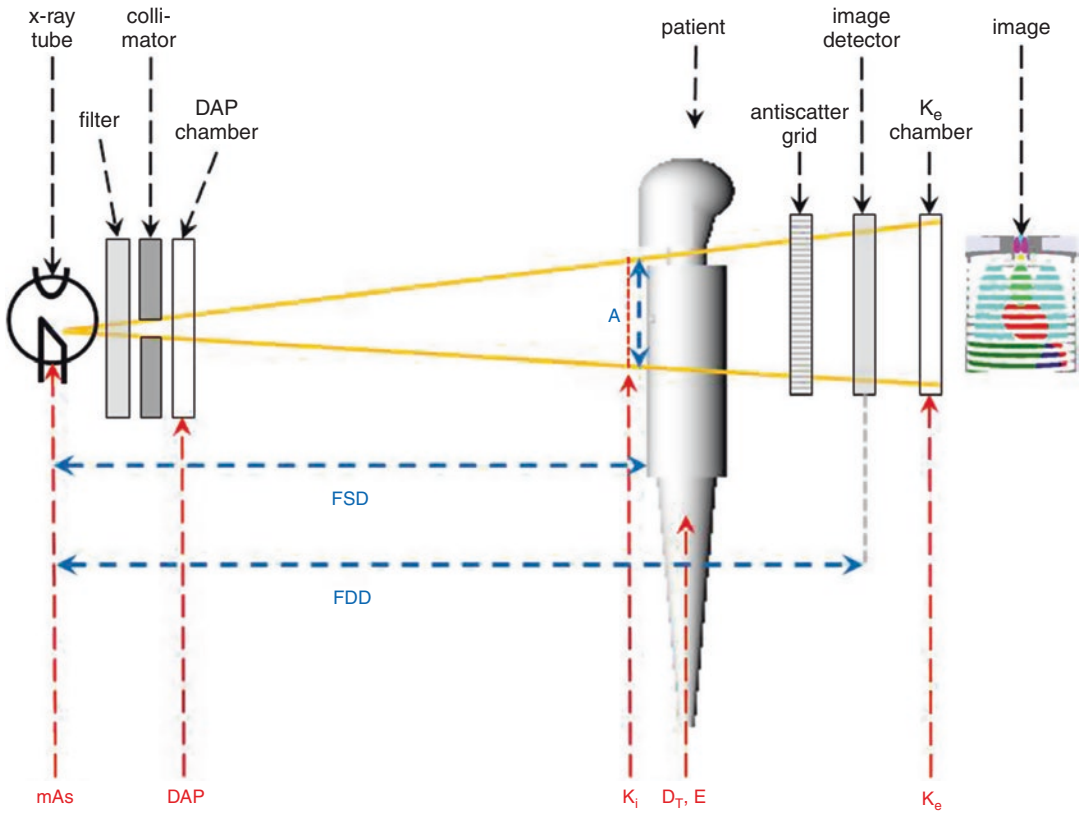

Fig. 4.1 Technical principle of an ap chest X-ray and dose indicators corresponding to the technical components of the X-ray unit. The pictures of phantom and X-ray image were taken from the user interface of the PCXMC software used for the calculations in this book [58, 59] (© M. Seidenbusch 2018). Dose indicators (red): mAs = mAs product; DAP = Dose area product; K_i = Incidence air kerma; D_T = Organ dose in tissue T; E = effective dose; K_e = Exit air kerma. Irradiation geometry (blue): FSD = Focus-to-skin distance; FDD = Focus-to-detector distance; A = Field size

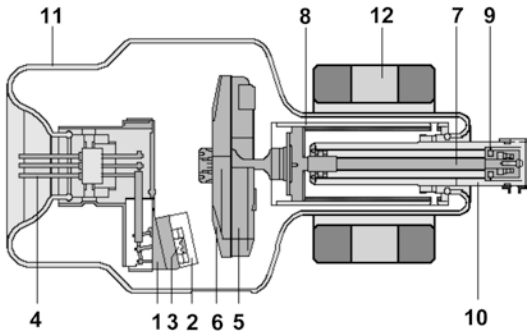

Fig. 4.2 Technical principle of an X-ray tube. (The picture of the X-ray tube is a modified picture from the book of *Hoxter* and *Schenz* [30].) (1) Cathode, (2) *Wehnelt* electrode, (3) Glow filaments, (4) High voltage connectors, (5) Rotating anode, (6) Focal track, (7) Molybdenum spindle, (8) Rotor, (9) Ball-bearing of the rotating anode, (10) Outer part of the rotating anode, (11) Bulb, (12) Stator

$$E_{\text{kin}} = e \cdot V \tag{4.1}$$

This kinetic energy is transformed into energy of bremsstrahlung that is released from the electrons during their slowing-down within the electric fields of the atomic nucleus of the anode material. As the slowing-down of electrons is a probabilistic process, bremsstrahlung will not have a defined energy but show an energy distribution which is called *bremsstrahlung spectrum* or *X-ray spectrum* with a maximum energy E_{max} which equals to the kinetic energy of the electrons:

$$E_{\text{max}} = E_{\text{kin}} \tag{4.2}$$

Typical X-ray spectra generated by diagnostic X-ray tubes when selecting a tube voltage of

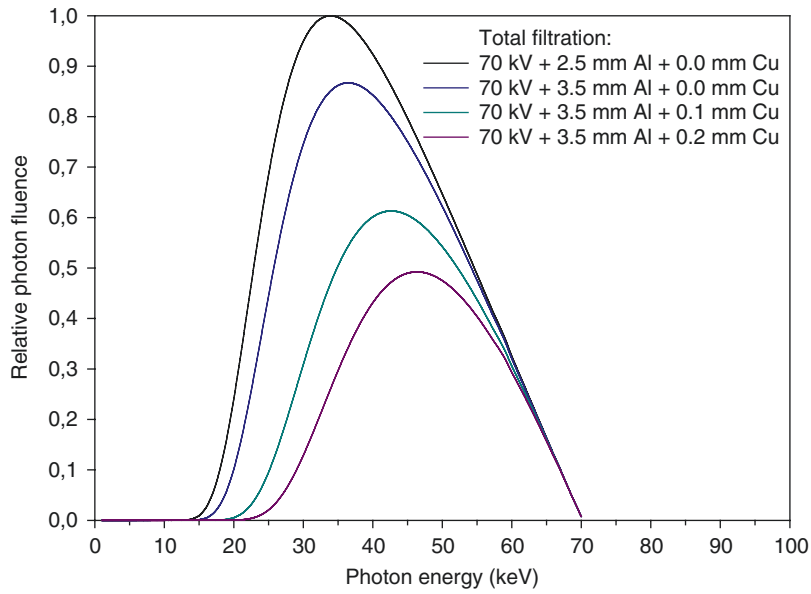

Fig. 4.3 X-ray spectra resulting from various total filtrations. The maximal photon energy is defined by the tube voltage and equals in this example to 70 keV. (From [53], © Springer Verlag 2015, courtesy Springer Verlag)

70 kV are depicted in Fig. 4.3. It should be stated here that the shape of X-ray spectra is also affected a little bit by the anode angle, but the contribution of the anode angle is to be neglected for practical clinical purposes.

The percentage of electric energy being transformed into radiation energy is called the *yield Y* of the X-ray tube. As the dose rate of an X-ray unit is proportional to the yield of the tube and the yield is proportional to the tube current, any kind of radiation dose quantity D is a linear function of the current-time product or mAs product:

$$D \sim Y \sim \text{mAs product} \tag{4.3}$$

However, as the yield of an X-ray tube must be known in order to estimate the dose rate of an X-ray tube from the tube current, the mAs product cannot be considered as an appropriate dose indicator for the reconstruction of organ and effective doses.

4.2.2 Filters and Total Filtration

X-ray spectra originating from X-ray tubes are composed of bremsstrahlung photons with an energy range from zero to the maximal photon energy defined by the tube voltage. As low energy X-rays are absorbed in the patient's skin surface and thus increase the patient's skin dose without contributing to the diagnostic imaging process, X-ray spectra originating from the X-ray tube should not be applied for X-ray diagnostics in their native form. However, the filtering of X-ray spectra by placing metallic filters between the X-ray tube and the patient will reduce the percentage of low energy photons and thus will reduce the exposure of the patient. The *total filtration* of an X-ray unit is defined as the sum of the *inherent filtration* of the X-ray tube and the *additional filtration* that can be added depending on the clinical situation. Figure 4.3 depicts various diagnostic X-ray spectra resulting from different total filtrations when selecting a tube voltage of 70 kV. As can be seen, an increasing total filtration goes along with a shift of the maximum of the X-ray spectrum towards higher photon energies but also with a decrease of the relative photon fluence and thus with a decrease of the dose rate. As a consequence, the tube current has to be increased when increasing the total filtration in order to achieve the same image detector dose.

4.2.3 Collimator

Collimation of the primary X-ray field originating from the X-ray tube to the anatomical region of interest is necessary when performing diagnostic X-ray examinations. Collimation has two effects: First, it is one of the most effective measures in order to reduce the radiation exposure of the patient. Second, reducing the irradiated patient volume will reduce the amount of scattered photons and thus reduce the image noise and therefore improve the image quality. Please note that by now collimating is the unique method in diagnostic radiology for optimizing radiation exposure and image quality simultaneously.

Depending on the patient's age and the clinical situation, optimal field sizes which can be achieved under optimal clinical conditions can be defined. In clinical application, field sizes are visually defined by harmonizing the boundaries of the light field with specific anatomical landmarks of the patient. However, small deviations of an optimal field collimation may considerably increase the field size (Fig. 4.4). Thus, not only optimal but also suboptimal field settings should be considered in dose calculations - one of the main concerns of this book.

Of course, uncertainties in the visual estimation of the radiation field through the light field do also play a role when defining the field size. A very important prerequisite for determining an optimal field size is, of course, that there is congruency of light field and radiation field [29]. Nevertheless, the field sizes applied during paediatric X-ray examinations have been found to differ considerably between different institutions and even within radiological departments [7, 18, 19, 23, 27, 29, 41, 56, 57, 60, 66].

4.2.4 KAP Meter

The KAP meter (synonymously: DAP chamber) is mounted at the X-ray unit after the collimation system and serves for measurement of the kerma area product (KAP) or dose area product

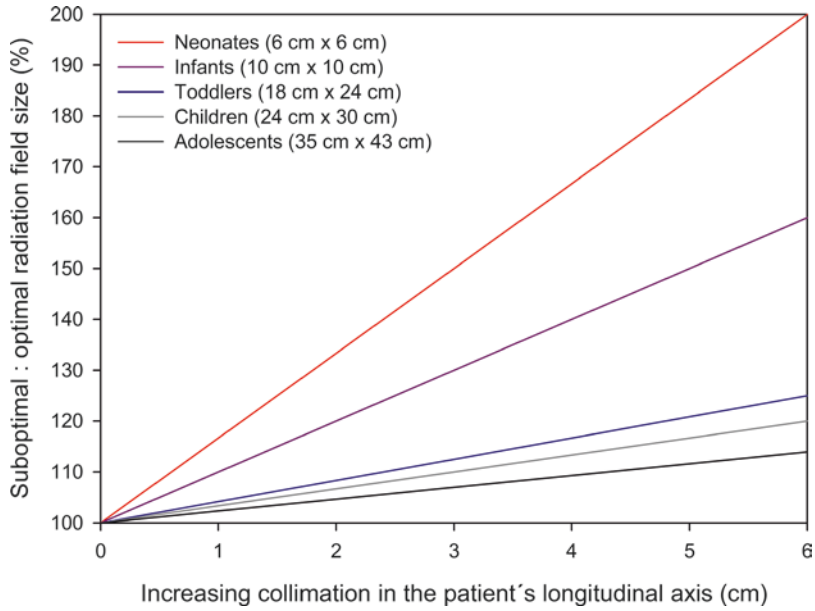

Fig. 4.4 Ratio of optimal and suboptimal field size of an ap/pa chest X-Ray due to additional increase of field size in longitudinal axis of the patient. Naturally, small optimal field sizes are applied in neonates and young infants and large optimal field sizes are applied in adolescents accordingly. Thus, an additional increase of field height due to suboptimal collimation in longitudinal direction will not considerably increase the field size in adolescents but will increase the field size in neonates and young infants by more than 100%. (From [53], © Springer Verlag 2015, courtesy Springer Verlag)

(DAP) (see Sect. 4.3.2) as a dose indicator for the radiation exposure of the patient. The dose area product is the most important dose quantity for the reconstruction of the organ and the effective doses achieved and thus for assessing radiation risks during conventional X-ray examinations [32].

In daily routine, no entrance surface dose will be measured but the dose area product. In Germany, recording of the dose measured during paediatric X-ray examinations is mandatory [63]. Especially in neonatology, dose meters must be sensitive enough in order to be able to measure entrance surface doses of 10 μGy or less. Highly sensitive dose meters are offered by several manufacturers of medical dosimetry systems which are, however, unable to capture all relevant dose quantities. It is particularly important in paediatric radiology that clinical KAP meters have been calibrated accurately [43].

4.2.5 Patient

The patient is the most variable component of the X-ray equipment in paediatric radiology as his diameter varies over a wide range depending on age group, beam projection, and body part to be examined. As X-rays are attenuated exponentially when passing through the patient, the radiation exposure of the patient is strongly affected by the patient's size and shape.

4.2.6 Antiscatter Grid

The purpose of antiscatter grids is to reduce scattered radiation originating from the patient and thus reducing image noise. Antiscatter grids consist of a system of lead lamellae that are aligned according to the irradiation geometry. Therefore, antiscatter grids have to be adjusted carefully considering the focus-to-detector distance. However, not only scattered radiation is absorbed by antiscatter grids but also a fraction of the useful beam. Thus, the use of antiscatter grids goes along dependent on patient age and type of X-ray examination with an increase of radiation exposure of the patient up to a factor of three to five [13]. Overall, the use of antiscatter grids in paediatric radiology is discussed controversial [3, 15, 24, 34, 48, 49]. Nevertheless, the authors of this book recommend using of antiscatter grids in paediatric X-ray examinations of children beyond the age of 8 years for chest X-rays (Fig. 4.5). For skull radiographs, an antiscatter grid is already used in infants. Details on the use of antiscatter grid were published in many guidelines (e.g. [15]).

4.3 Dose Quantities

In this section, dose quantities as being used in this book shall be presented short from the clinical point of view. For more precise physical definitions, see e.g. the books of *Attix* [5] or *Jones* and *Cunningham* [40].

The interaction between ionizing radiation and material can be divided into four phases [46]: The physical phase of first order, the physical phase of second order and the physico-chemical and biological phase. In the physical phase of first order, radiation energy from the incident X-ray beam is transferred into kinetic energy of secondary electrons through the photo effect, the *Compton* effect, and the pair formation effect. In the physical phase of second order, the kinetic energy of the secondary electrons is absorbed in matter, generating ions and radicals in the chemical phase. Ions and radicals cause chemical reactions in material, as well as radiation damages like DNA strand brakes in biological environment during the biological phase of radiation interaction. To each of these phases, a dose quantity can be attributed: the Kerma (Kerma = kinetic energy released in material) to the physical phase of first order, the absorbed dose (synonymously: energy dose) to the physical phase of second order, the equivalent dose to the chemical phase, and the effective dose to the biological phase. Figure 4.6 depicts the four phases of radiation interaction with matter and the dose quantities associated.

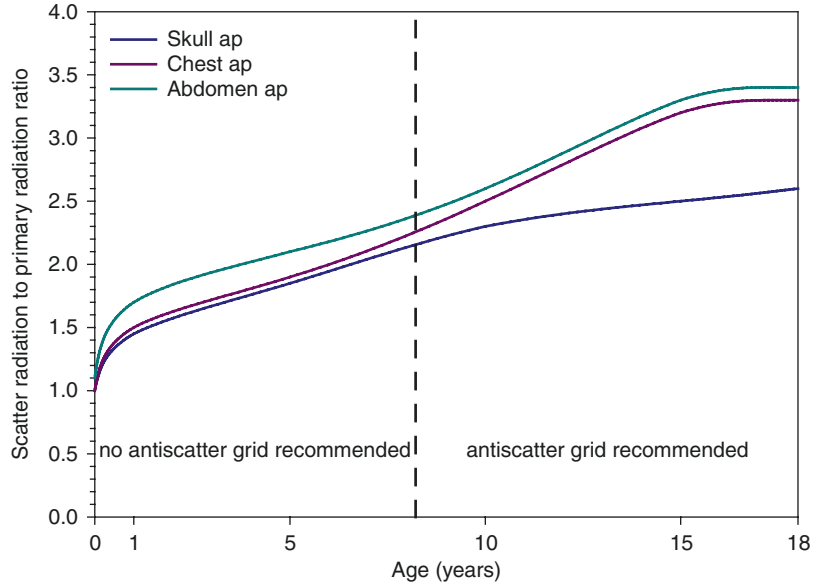

Fig. 4.5 Ratio of scatter radiation to primary radiation as a function of patient age and type of X-ray examination (using the scatter ratios of *Bushberg* et al. [13]). The ratio of scatter is highest for abdominal X-rays even in early childhood. As could be expected, the fraction of scattered radiation is increasing with age for chest and abdominal X-rays. For the skull, the slope of scatter curve decreases during adolescence. According to these data, an antiscatter grid is recommended for all X-rays in children older than 8 years of age. (© M. Seidenbusch 2018)

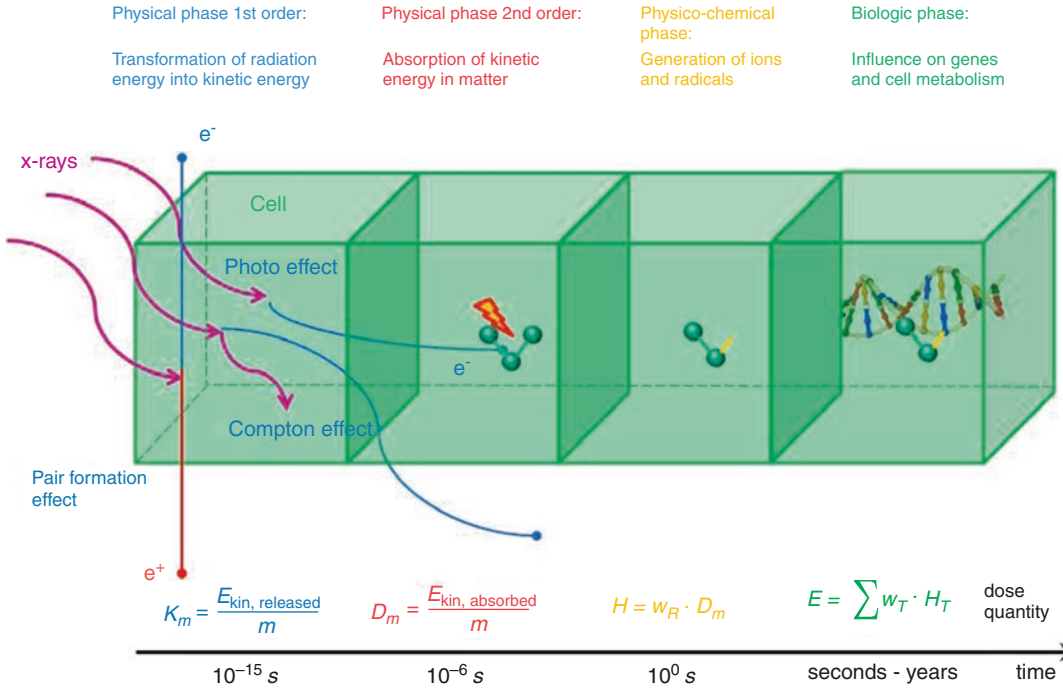

Fig. 4.6 The four phases of radiation interaction with living matter [46] and corresponding dose quantities. Green cubes symbolize living cells. Purple arrows symbolize X-ray photons, blue and red lines secondary electrons (e^-) and secondary positrons (e^+), respectively. The four phases of interaction are depicted in chronological order in four cells. For details, see the text. (© M. Seidenbusch 2018)

Table 4.1 Backscatter factors B for various radiation qualities, field sizes, and focus-to-skin distances [45]

	Total filtration F				Backscatter factor B for ICRU tissue		
Voltage U (kV)	Al (mm)	Cu (mm)	HVL (mm)	Mean energy (keV)	10 × 10 cm^2	20 × 20 cm^2	25 × 25 cm^2
50	**2.5**	**–**	1.74	32.0	1.25	1.27	1.28
60	**2.5**	**–**	2.08	35.8	1.28	1.32	1.32
70	**2.5**	**–**	2.41	39.3	1.31	1.36	1.36
	3.0	**–**	2.64	40.0	1.32	1.37	1.38
	3.0	**0.1**	3.96	44.0	1.39	1.47	1.47
80	**2.5**	**–**	2.78	42.9	1.33	1.39	1.39
	3.0	**–**	3.04	43.7	1.34	1.40	1.41
	3.0	**0.1**	4.55	48.2	1.40	1.50	1.51
90	**2.5**	**–**	3.17	46.3	1.34	1.41	1.42
	3.0	**–**	3.45	47.0	1.36	1.43	1.44
	3.0	**0.1**	5.12	51.7	1.41	1.51	1.53
100	**2.5**	**–**	3.24	48.1	1.34	1.41	1.42
	3.0	**–**	3.88	50.0	1.37	1.45	1.46
	3.0	**0.1**	5.65	54.8	1.42	1.53	1.55
120	**2.5**	**–**	–	–	–	–	–
	3.0	**–**	4.73	55.4	1.38	1.45	1.49
	3.0	**0.1**	6.62	60.1	1.42	1.54	1.56
150	**2.5**	**–**	4.79	59.1	1.36	1.46	1.48
	3.0	**–**	6.80	64.9	1.39	1.51	1.53
	3.0	**0.1**	8.50	69.2	1.41	1.54	1.57

Annotations: HVL = half value length of the X-rays of a certain radiation quality

4.3.1 Kerma

If material M is hit by an X-ray photon field, secondary electrons are released within the material by the photoelectric effect, by the *Compton* effect, and by the pair formation effect. The amount of the radiation energy of the incident photon field that is transferred to kinetic energy E_{kin} of secondary electrons within a given mass element m is named the *kerma* (KERMA = kinetic energy released in material) K_{M}:

$$K_{\text{M}} = \frac{dE_{\text{kin}}}{dm} \tag{4.4}$$

The physical SI[1] unit of the kerma is 1 Gray = 1 Gy = 1 J kg^{-1}.

The *incidence air kerma* K_i is defined as the kerma in air in the entrance plane of the incident radiation field at a patient's position but without presence of the patient:

$$K_i = K_{\text{air}} \tag{4.5}$$

When a patient is present, the corresponding dose quantity is the *entrance surface dose* K_{s} that is defined as the sum of incidence air kerma and the backscatter radiation from the patient. The entrance surface dose can be calculated by multiplying the incidence air kerma with a *backscatter factor B*:

$$K_{\text{s}} = B \cdot K_i \tag{4.6}$$

Backscatter factors depend on the parameters of the beam quality (X-ray tube voltage V and total filtration F [12]) and the parameters of the beam geometry (beam projection p, field size A, and focus-to-skin distance FSD):

$$B = B\left(V, F, p, A, \text{FSD}\right) \tag{4.7}$$

Backscatter factors for diagnostic photon energies and various field sizes and focus-to-film distances are given in [45] and are provided in Table 4.1 and Fig. 4.7.

4.3.2 Dose Area Product (DAP), Kerma Area Product (KAP)

The *Dose Area Product (DAP)* or strictly speaking: *air Kerma Area Product* (KAP) [32, 42] is the product of incident air kerma K_i at any given

[1] SI = Système international d'unités.

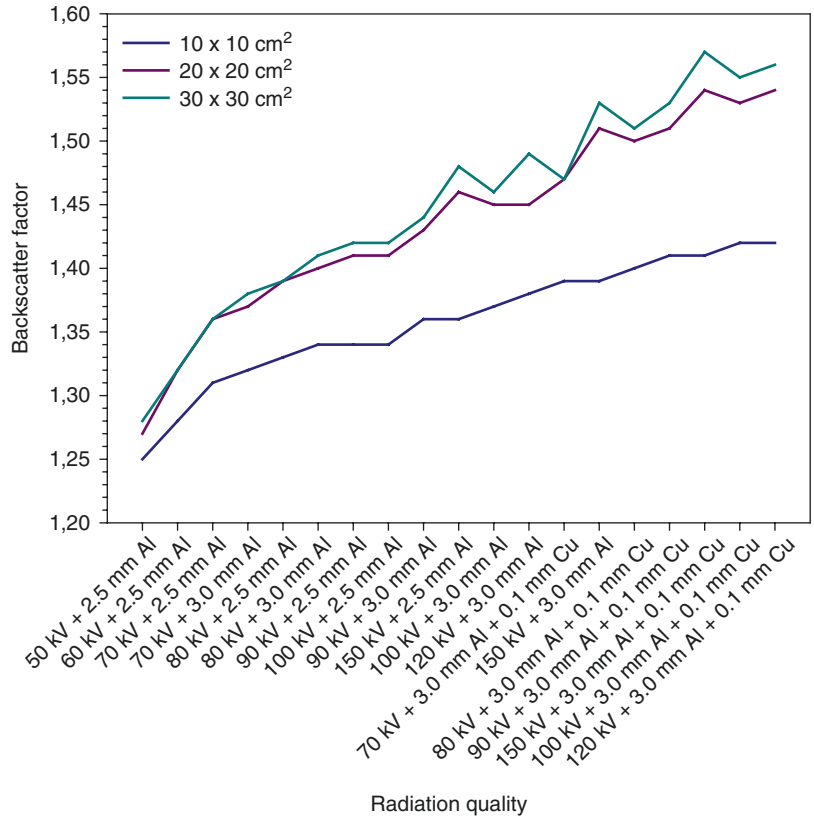

Fig. 4.7 Backscatter factors for various radiation qualities and field sizes. Visualization of the data in Table 4.1. Generally, backscatter factors go up with increasing effective energy of the radiation field. (© M. Seidenbusch 2018)

Table 4.2 Conversion coefficients *C* for various DAP measuring units

	mR cm²	cR cm²	dR cm²	R cm²	mGy cm²	cGy cm²	µGy m²	$B = A/C$
mR cm²	1	0.1	0.01	0.001	0.0084	0.00084	0.00084	
cR cm²	10	1	0.1	0.01	0.084	0.0084	0.0084	
dR cm²	100	10	1	0.1	0.84	0.084	0.084	
R cm²	1000	100	10	1	8.4	0.84	0.84	
mGy cm²	119	11.9	1.19	0.119	1	0.1	0.1	
cGy cm²	1190	119	11.9	1.19	10	1	1	
µGy m²	1190	119	11.9	1.19	10	1	1	
$A = C\,B$	C							

Note that DAP values in column A can be calculated from DAP values in row B by the equation $A = C\,B$ and vice versa

point of the X-ray beam and the field size A at this point:

$$\mathrm{KAP} = \mathrm{DAP} = K_i \cdot A \tag{4.8}$$

The physical SI unit of the dose area product is 1 Gy m².

As an X-ray source is usually a point source, the inverse square law is valid for the irradiation geometry, and the dose area product remains nearly constant over the whole focus-to-skin distance. Furthermore, the dose area product is a dose indicator which represents a measure of the radiation exposure of the patient. The dose area product is usually measured by an ionization chamber that is fixed at the beam collimator.

In diagnostic radiology, there are various dose measuring units in practical use for the DAP as shown in Table 4.2. Table 4.2 provides conversion coefficients C for transforming the DAP measuring units into each other.

4.3.3 Absorbed Dose

The part E of kinetic energy of secondary electrons E_{kin} that is transferred to a mass element m of a material M is named the *absorbed dose* (in Europe synonymously: *energy dose*) D_M:

$$D_M = \frac{dE}{dm} \tag{4.9}$$

The physical SI unit of the absorbed or energy dose is 1 Gray = 1 Gy = 1 J kg^{-1}.

In case of secondary electron equilibrium which can be assumed to be always achieved in the photon energy range of X-ray diagnostics, the absorbed dose equals the kerma.

If an absorbed dose or energy dose is estimated for an organ or tissue T, the absorbed dose or energy dose is also called *organ absorbed dose* (in Europe synonymously: *organ energy dose*) D_T:

$$D_T = D_M \text{ achieved in tissue T} \tag{4.10}$$

4.3.4 Equivalent Dose

In order to allow for the fact that different radiation qualities differ in energy transfer mechanisms, the *equivalent dose* H_M can be calculated from an absorbed or energy dose by multiplying the absorbed or energy dose D_M with a radiation-specific *radiation weighting factor* w_R (almost synonymously: *quality factor* Q) as follows:

$$H_M = w_R \cdot D_M = Q \cdot D_M \tag{4.11}$$

The physical SI unit of the equivalent dose is 1 Sievert = 1 Sv = 1 J kg^{-1}.

Within the photon energy range applied in X-ray diagnostics, the radiation weighting factor has been defined to be $w_R = 1$.

If an equivalent dose is estimated for an organ or tissue T, the equivalent dose is also called *organ equivalent dose* or, in short, *organ dose* H_T:

$$H_T = H_M \text{ achieved in tissue T} \tag{4.12}$$

Note that the organ dose is defined as the average dose achieved within an organ or tissue.

4.3.5 Effective Dose

In order to allow for the fact that different organs and tissues T differ in radiation sensitivity, the *effective dose E* has been defined as the weighted sum of all organ doses, each of them weighted with a tissue-specific *tissue weighting factor* w_T representing the specific radiation sensitivity of organs and tissues T as follows:

$$H_T = \sum_T w_T \cdot H_T \tag{4.13}$$

The physical SI unit of the effective dose is 1 Sievert = 1 Sv = 1 J kg^{-1}.

As the effective dose is intended to represent the virtual whole body dose that would have to be achieved in order to cause the same stochastic risk as a really applied dose distribution in some organs or tissues, the condition

$$\sum_T w_T = 1 \tag{4.14}$$

has to be fulfilled when defining the tissue weighting factors w_T. For this reason, the effective dose has sometimes also been called the "weighted sum of stochastic risks". However, the effective dose has been intended to serve as a risk indicator in occupational health and has not been defined for describing the radiation exposure of patients originally [39], particularly not for children. Therefore, its application for describing radiation exposure of patients in diagnostic radiology has to be estimated critically [14, 21, 22]. Although attempts have been made to derive tissue weighting factors for children [2, 8, 44] in recent years, the concept of effective dose ought to be considered as to be inapplicable for paediatric patients at least in the opinion of the authors of this book.

4.4 Dose Reconstruction Algorithms

Reconstruction of the organ and the effective doses achieved during conventional X-ray examinations can be performed through various mathematical methods [1, 20]. In recent years, the conversion